Journal of Computational and Applied Mathematics 371 (2020) 112700

Contents lists available at ScienceDirect

Journal of Computational and Applied Mathematics

journal homepage: www.elsevier.com/locate/cam

Adaptive discontinuous Galerkin methods for solving an incompressible Stokes flow problem with slip boundary condition of frictional type

Fei Wang [a,*,1], Min Ling [b], Weimin Han [b,c,2], Feifei Jing [d,3]

[a] School of Mathematics and Statistics & State Key Laboratory of Multiphase Flow in Power Engineering, Xi'an Jiaotong University, Xi'an, Shaanxi 710049, China
[b] School of Mathematics and Statistics, Xi'an Jiaotong University, Xi'an, Shaanxi 710049, China
[c] Department of Mathematics & Program in Applied Mathematical and Computational Sciences, University of Iowa, Iowa City, IA 52242, USA
[d] School of Mathematics and Statistics & Xi'an Key Laboratory of Scientific Computation and Applied Statistics, Northwestern Polytechnical University, Xi'an 710129, China

A R T I C L E I N F O

Article history:
Received 30 March 2019
Received in revised form 26 October 2019

MSC:
65N30
49J40

Keywords:
Discontinuous Galerkin methods
Variational inequality
Stokes equations
Slip boundary condition
A posteriori error analysis

A B S T R A C T

We consider the numerical solution of a variational inequality arising in the study of an incompressible Stokes flow with a nonlinear slip boundary condition of frictional type. We study several discontinuous Galerkin (DG) schemes for solving the problem, and derive reliable and efficient residual type a posteriori error estimators. An adaptive DG method is constructed based on the error estimators to solve the problem. Some numerical examples are presented to illustrate the efficiency of the adaptive DG method.

1. Introduction

The Navier–Stokes (NS) equations describe the motion of a viscous fluid and are widely applied in physics and engineering, such as modeling of ocean currents, design of hydroelectric power stations, analysis of pollutions, and so on. For a complete description of a problem in fluid dynamics, the NS equations are supplemented by appropriate boundary conditions, which is one of the most important factors determining the behavior of the fluid. In most research papers and textbooks on classical hydrodynamics, only the no-slip boundary condition is considered, i.e., there is no relative motion on the fluid–solid interface. The validity of the no-slip boundary condition has been widely debated since the 19th century, and there has been no universal agreement on the nature of the boundary condition in hydrodynamics [1]. In the past

* Corresponding author.
E-mail addresses: feiwang.xjtu@xjtu.edu.cn (F. Wang), lingmin@stu.xjtu.edu.cn (M. Ling), weimin-han@uiowa.edu (W. Han), ffjing@nwpu.edu.cn (F. Jing).

1 The work of this author was partially supported by the National Natural Science Foundation of China (Grant No. 11771350).
2 The work of this author was partially supported by NSF under grant DMS-1521684.
3 The work of this author was supported by the Natural Science Fundation of Shaanxi Province (Grant No. 2019JQ-173) and Fundamental Research Funds for the Central Universities of China (Grant No. 31020180QD078).

https://doi.org/10.1016/j.cam.2019.112700
0377-0427/

several decades, through more experiments done with advanced measurement techniques, the assumption of no-slip boundary condition has been challenged [1,2]. Slip phenomena have been observed in many applications, for examples, blood flow [3], polymer–polymer welding and sliding phenomena [4], fluid slipping on super-hydrophobic surface [2], gaseous slip flow in a long micro-channels [5].

To describe the slip phenomena, some physical models have been proposed and studied, such as slip length model [6] (the tangent component of the fluid velocity is proportional to the shear rate on the surface), stagnant layer model [7], contact line motion [8], and so on. For a historical account of the development of the slip and no-slip boundary conditions, we refer the reader to [1,2] and the references therein. Recently, some investigations with modern techniques [9–12] show more evidence of the slip phenomena. In particular, some experiments [11–13] indicate that the slip occurs when the shear stress reaches a threshold determined by properties of the fluid and the materials of solid surface. In the lectures [14] delivered at College de France in 1993, Fujita introduced a slip boundary condition of frictional type for applications in blood flow and polymer–polymer sliding phenomena. This type of slip boundary condition can model the slip and no-slip phenomena simultaneously. The boundary conditions of these problems are subdifferentiable, leading to variational inequalities (VIs). The variational inequality problem governed by the NS (or Stokes) equations is difficult to solve numerically due to the slip boundary condition in inequality form, nonlinearity of the convection term, and the mixed form of the velocity and the pressure variables. The well-posedness of these problems has been studied in [15–22]. In [23–29], numerical methods for solving these NS (or Stokes) VI problems are investigated.

In the past four decades, discontinuous Galerkin (DG) methods have been developed for solving various differential equations in virtue of the flexibility in constructing feasible local shape function spaces as well as the capability to capture non-smooth or oscillatory solutions effectively. The DG methods discretize equations element by element, and exchange information between neighboring elements through numerical traces, so that the methods are locally conservative, which is a very important feature for good numerical methods. Because inter-element continuity is not required in the function spaces, DG methods can easily handle general meshes with hanging nodes and elements of different shapes, so they are suitable for adaptive mesh refinement. Moreover, locality of the discretization makes the DG methods ideally suited for parallel computing (see [30–32] and the references therein). The discontinuous Galerkin methods have been developed and studied for solving the Navier–Stokes equations, e.g. [33–37] and the reference therein. Due to many advantages, recently, DG methods have been applied for solving variational inequalities [38–46]. One major weakness of the DG methods is that more degree of freedom is needed. To reduce the computational cost, it is natural to develop adaptive DG algorithms based on a posteriori error estimates of DG methods for VIs [47–51].

In this paper, we study discontinuous Galerkin (DG) methods for numerically solving variational inequalities controlled by Stokes equations with the slip boundary condition of frictional type. To solve the Stokes (or NS) equations, compared with the standard finite element method, DG methods can be more stable and accurate. DG methods are locally conservative by design, and can capture discontinuous physical quantities. We study a posteriori error estimates to derive reliable and efficient residual type error estimators for implementing adaptive DG algorithm, so that we can solve the problems with higher precision under existing hardware conditions.

The paper is organized as follows. In Section 2, we introduce the Stokes flow with slip boundary condition and its variational inequality formulation. Then we present four DG formulations for solving the variational inequality and show the consistency of the schemes in Section 3. We provide a posteriori error analysis for the scheme in Section 4. To prove the reliability of the error estimators, we construct a conforming divergence free solution from the DG solution, and show the efficiency of the local error estimator as well. In the last section, we present some numerical examples to compare the DG solutions from adaptive meshes and those from uniformly refined meshes.

2. Variational inequality controlled by incompressible Stokes equations

2.1. Stokes flow with slip boundary condition

Let $\Omega \subset \mathbb{R}^d$, $d = 2, 3$, be a simply connected polygonal/polyhedral domain with a Lipschitz boundary Γ that is divided into two parts $\overline{\Gamma_D}$ and $\overline{\Gamma_S}$ such that Γ_D and Γ_S are relatively open and mutually disjoint with meas$(\Gamma_D) > 0$. Denote by $\boldsymbol{u} : \Omega \to \mathbb{R}^d$ a velocity field. The linearized strain rate tensor

$$\boldsymbol{\varepsilon}(\boldsymbol{u}) = \frac{1}{2}\,(\nabla \boldsymbol{u} + (\nabla \boldsymbol{u})^T)$$

and the Cauchy stress

$$\boldsymbol{T} = 2\,\nu\,\boldsymbol{\varepsilon}(\boldsymbol{u}) - p\mathbf{I} \tag{2.1}$$

are second order symmetric tensors, which take values in $\mathbb{S}^d$, the space of second order symmetric tensors on $\mathbb{R}^d$ with the inner product $\boldsymbol{T} : \boldsymbol{U} = \sum_{i,j=1}^{d} T_{ij}U_{ij}$ and norm $\|\boldsymbol{U}\| = (\boldsymbol{U} : \boldsymbol{U})^{\frac{1}{2}}$. Here, $\mathbf{I}$ is the identity tensor, p is the pressure, and ν is the viscosity of the fluid. Let $\boldsymbol{n}$ be the unit outward normal to Γ. For a vector $\boldsymbol{v}$, denote its normal component and tangential component by $v_n = \boldsymbol{v}\cdot\boldsymbol{n}$ and $\boldsymbol{v}_\tau = \boldsymbol{v} - v_n\boldsymbol{n}$ on the boundary. Similarly for a tensor-valued function $\boldsymbol{T}$, we define its normal component $T_n = (\boldsymbol{T}\boldsymbol{n})\cdot\boldsymbol{n}$ and tangential component $\boldsymbol{T}_\tau = \boldsymbol{T}\boldsymbol{n} - T_n\boldsymbol{n}$. We have the decomposition formula

$$(\boldsymbol{T}\boldsymbol{n})\cdot\boldsymbol{v} = (T_n\boldsymbol{n} + \boldsymbol{T}_\tau)\cdot(v_n\boldsymbol{n} + \boldsymbol{v}_\tau) = T_n v_n + \boldsymbol{T}_\tau\cdot\boldsymbol{v}_\tau.$$

In this paper, we consider the Stokes problem for a viscous incompressible fluid with a slip boundary condition of frictional type. The Stokes equations are

$$\begin{cases} -\mathrm{div}(2\nu\boldsymbol{\varepsilon}(\boldsymbol{u}))+\nabla p = \boldsymbol{f} & \text{in } \Omega, \\ \mathrm{div}\,\boldsymbol{u} = 0 & \text{in } \Omega. \end{cases} \tag{2.2}$$

On the boundary Γ_D, we impose the homogeneous Dirichlet boundary condition

$$\boldsymbol{u}=\boldsymbol{0} \quad \text{on } \Gamma_D. \tag{2.3}$$

On the boundary Γ_S, we impose no-leak boundary condition

$$u_n = 0 \quad \text{on } \Gamma_S, \tag{2.4}$$

and slip boundary condition

$$|\boldsymbol{T}_\tau| \le g, \quad \boldsymbol{T}_\tau\cdot\boldsymbol{u}_\tau + g|\boldsymbol{u}_\tau| = 0 \quad \text{on } \Gamma_S. \tag{2.5}$$

Note that the slip boundary condition is equivalent to the following relation:

$$|\boldsymbol{T}_\tau| \le g, \quad |\boldsymbol{T}_\tau| < g \Rightarrow \boldsymbol{u}_\tau = \boldsymbol{0}, \quad \boldsymbol{u}_\tau \ne \boldsymbol{0} \Rightarrow \boldsymbol{T}_\tau = -g\,\boldsymbol{u}_\tau/|\boldsymbol{u}_\tau| \quad \text{on } \Gamma_S. \tag{2.6}$$

For the source term, assume

$$\boldsymbol{f} \in [L^2(\Omega)]^d, \tag{2.7}$$

and for the friction bound function, assume

$$g \in L^\infty(\Gamma_S), \quad g > 0 \text{ a.e. on } \Gamma_S. \tag{2.8}$$

2.2. The variational inequality formulation

We introduce a Hilbert space

$$\boldsymbol{V} = \{\boldsymbol{v} \in [H^1(\Omega)]^d : \boldsymbol{v} = \boldsymbol{0} \text{ a.e. on } \Gamma_D,\ v_n = 0 \text{ a.e. on } \Gamma_S\} \tag{2.9}$$

with the inner product and norm defined by

$$(\boldsymbol{u},\boldsymbol{v})_V = 2\nu\int_\Omega \boldsymbol{\varepsilon}(\boldsymbol{u}) : \boldsymbol{\varepsilon}(\boldsymbol{v})\,dx, \quad \|\boldsymbol{v}\|_V = \sqrt{(\boldsymbol{v},\boldsymbol{v})_V}.$$

Since $\mathrm{meas}(\Gamma_D) > 0$, we know that $\|\cdot\|_V$ is equivalent to the standard $[H^1(\Omega)]^d$ norm on $\boldsymbol{V}$ by Korn's inequality [52]. Let

$$Q = L_0^2(\Omega) = \left\{q \in L^2(\Omega) : \int_\Omega q(\boldsymbol{x})\,dx = 0\right\}.$$

To provide a variational formulation of the problem (2.2)–(2.5), we multiply the two equations in (2.2) by $\boldsymbol{w} \in \boldsymbol{V}$ and $q \in Q$, respectively, integrate on Ω, and apply the following integration by parts formula over a Lipschitz domain D:

$$\int_D \mathrm{div}\,\boldsymbol{T}\cdot\boldsymbol{w}\,dx = \int_{\partial D}\boldsymbol{T}\boldsymbol{n}\cdot\boldsymbol{w}\,ds - \int_D \boldsymbol{T} : \boldsymbol{\varepsilon}(\boldsymbol{w})\,dx \tag{2.10}$$

to get

$$\begin{cases} 2\nu\int_\Omega \boldsymbol{\varepsilon}(\boldsymbol{u}) : \boldsymbol{\varepsilon}(\boldsymbol{w})dx - \int_\Omega p\,\mathrm{div}\,\boldsymbol{w}dx - \int_\Gamma \boldsymbol{T}\boldsymbol{n}\cdot\boldsymbol{w}\,ds = (\boldsymbol{f},\boldsymbol{w}) & \forall\,\boldsymbol{w}\in\boldsymbol{V}, \\ -\int_\Omega q\,\mathrm{div}\,\boldsymbol{u}dx = 0 & \forall\,q \in Q. \end{cases} \tag{2.11}$$

Let $\boldsymbol{w} = \boldsymbol{v}-\boldsymbol{u}$ in the first equation. By applying the boundary condition (2.3)–(2.5), we have

$$-\int_\Gamma \boldsymbol{T}\boldsymbol{n}\cdot(\boldsymbol{v}-\boldsymbol{u})\,ds = \int_{\Gamma_S}\boldsymbol{T}_\tau\cdot(\boldsymbol{u}_\tau-\boldsymbol{v}_\tau)\,ds \le \int_{\Gamma_S}(\boldsymbol{T}_\tau\cdot\boldsymbol{u}_\tau + |\boldsymbol{T}_\tau|\,|\boldsymbol{v}_\tau|)\,ds \le \int_{\Gamma_S}(g|\boldsymbol{v}_\tau| - g|\boldsymbol{u}_\tau|)\,ds.$$

Therefore, the variational formulation of the Stokes problem with the slip boundary condition of frictional type reads as follows: Find $(\boldsymbol{u},p) \in \boldsymbol{V}\times Q$ such that

$$\begin{cases} a(\boldsymbol{u},\boldsymbol{v}-\boldsymbol{u}) + b(\boldsymbol{v}-\boldsymbol{u},p) + j(\boldsymbol{v}_\tau) - j(\boldsymbol{u}_\tau) \ge (\boldsymbol{f},\boldsymbol{v}-\boldsymbol{u}) & \forall\,\boldsymbol{v}\in\boldsymbol{V}, \\ b(\boldsymbol{u},q) = 0 & \forall\,q\in Q, \end{cases} \tag{2.12}$$

where

$$a(\boldsymbol{u},\boldsymbol{v}) := 2\nu\int_\Omega \boldsymbol{\varepsilon}(\boldsymbol{u}) : \boldsymbol{\varepsilon}(\boldsymbol{v})\,dx, \qquad b(\boldsymbol{v},q) := -\int_\Omega q\,\mathrm{div}\,\boldsymbol{v}dx,$$

$$j(\boldsymbol{v}_\tau) := \int_{\Gamma_S} g|\boldsymbol{v}_\tau|\, ds, \qquad (\boldsymbol{f}, \boldsymbol{v}) := \int_\Omega \boldsymbol{f}\cdot\boldsymbol{v}\, dx.$$

Remark 2.1. In most papers on the NS (or Stokes) flow with slip boundary condition of frictional type, the classical Stokes operator is used, i.e., (2.2) takes the form

$$\begin{cases} -\nu\Delta\boldsymbol{u} + \nabla p = \boldsymbol{f} & \text{in } \Omega, \\ \operatorname{div}\boldsymbol{u} = 0 & \text{in } \Omega. \end{cases}$$

This form of the Stokes equations is theoretically important, and is equivalent to (2.2) when the pure homogeneous Dirichlet boundary condition (no-slip boundary condition) is used. However, for the Stokes problem with the slip boundary condition, the original Stokes formulation (2.2) should be used.

2.3. Lagrangian multiplier associated with the frictional term

There exists a Lagrange multiplier $\boldsymbol{\lambda}_\tau \in [L^\infty(\Gamma_S)]^d$ such that [25,53]

$$\begin{cases} a(\boldsymbol{u},\boldsymbol{v}) + b(\boldsymbol{v},p) + \int_{\Gamma_S} g\,\boldsymbol{\lambda}_\tau\cdot\boldsymbol{v}_\tau\, ds = (\boldsymbol{f},\boldsymbol{v}) & \forall\, \boldsymbol{v}\in\boldsymbol{V}, \\ b(\boldsymbol{u},q) = 0 & \forall\, q\in Q, \\ |\boldsymbol{\lambda}_\tau| \le 1, \quad \boldsymbol{\lambda}_\tau\cdot\boldsymbol{u}_\tau = |\boldsymbol{u}_\tau| & \text{a.e. on } \Gamma_S. \end{cases} \tag{2.13}$$

For any $\boldsymbol{v}\in\boldsymbol{V}$, set

$$\ell(\boldsymbol{v}) = \int_\Omega \boldsymbol{f}\cdot\boldsymbol{v}\, dx - \int_{\Gamma_S} g\,\boldsymbol{\lambda}_\tau\cdot\boldsymbol{v}_\tau\, ds.$$

Then the first equation of (2.13) can be rewritten as

$$a(\boldsymbol{u},\boldsymbol{v}) + b(\boldsymbol{v},p) = \ell(\boldsymbol{v}) \quad \forall\, \boldsymbol{v}\in\boldsymbol{V}. \tag{2.14}$$

From (2.14), we can derive that

$$\boldsymbol{T}_\tau = -g\,\boldsymbol{\lambda}_\tau \quad \text{on } \Gamma_S. \tag{2.15}$$

For a decomposition $\mathcal{T}_h$ of Ω and a Lipschitz subdomain $\omega\subset\Omega$, define

$$\|\boldsymbol{v}\|_{\omega,V} = \sqrt{(\boldsymbol{v},\boldsymbol{v})_{\omega,V}} \quad \text{with } (\boldsymbol{u},\boldsymbol{v})_{\omega,V} = 2\nu\sum_{K\in\mathcal{T}_h}\int_{\omega\cap K}\boldsymbol{\varepsilon}(\boldsymbol{u}):\boldsymbol{\varepsilon}(\boldsymbol{v})\, dx,$$

and

$$|\boldsymbol{\lambda}_\tau|_{*,\gamma,\omega} := \sup_{0\ne\boldsymbol{v}\in[H_K^1(\omega)]^d}\frac{\int_\gamma g\,\boldsymbol{\lambda}_\tau\cdot\boldsymbol{v}_\tau\, ds}{\|\boldsymbol{v}\|_{\omega,V}},$$

where $\gamma\subset\partial\omega\cap\Gamma_S$ is a measurable subset and

$$[H_K^1(\omega)]^d = \{\boldsymbol{v}\in[L^2(\omega)]^d : \boldsymbol{v}|_{K\cap\omega}\in[H^1(K\cap\omega)]^d\}.$$

If $\omega=\Omega$, we use $\|\boldsymbol{v}\|_{h,V}$ instead of $\|\boldsymbol{v}\|_{\Omega,V}$, and the subscript ω is omitted. We claim that

$$|\boldsymbol{\lambda}_\tau|_{*,\Gamma_S} \lesssim (\|\boldsymbol{w}\|_{h,V} + \|y\|), \tag{2.16}$$

where $(\boldsymbol{w},y)$ is the solution of the auxiliary problem

$$\begin{cases} a(\boldsymbol{w},\boldsymbol{v}) + b(\boldsymbol{v},y) = \int_{\Gamma_S} g\,\boldsymbol{\lambda}_\tau\cdot\boldsymbol{v}_\tau\, ds & \forall\, \boldsymbol{v}\in\boldsymbol{V}, \\ b(\boldsymbol{w},q) = 0 & \forall\, q\in Q. \end{cases}$$

Here, the abbreviation $a\lesssim b$ stands for the inequality $a\le Cb$, where $C>0$ denotes a constant, which may take different values at different occurrences. By the boundedness of the bilinear form, it is easy to check that

$$\int_{\Gamma_S} g\,\boldsymbol{\lambda}_\tau\cdot\boldsymbol{v}_\tau ds \lesssim (\|\boldsymbol{w}\|_{h,V} + \|y\|)\|\boldsymbol{v}\|_{h,V},$$

which implies the inequality (2.16).

3. DG methods for the Stokes VI problem

3.1. Notation

For brevity, let us focus on the study of the problem for the 2 dimensional case, although the discussion can be extended to the 3-d problem similarly. For a bounded domain $D \subset \mathbb{R}^2$ and an integer $m \geq 0$, $H^m(D)$ is the Sobolev space with the usual norm $\|\cdot\|_{m,D}$ and semi-norm $|\cdot|_{m,D}$. When $m = 0$ and $D = \Omega$, the subscript 0 and Ω are omitted, i.e., $\|\cdot\|$ denote the $L^2(\Omega)$ norm. Let $\boldsymbol{u} = (u_1, u_2)^T \in [H^m(D)]^2$ and define its norm and semi-norm by $\|\boldsymbol{u}\|^2_{m,D} = \sum_{i=1,2} \|u_i\|^2_{m,D}$ and $|\boldsymbol{u}|^2_{m,D} = \sum_{i=1,2} |u_i|^2_{m,D}$, respectively. The space $[L^2(D)]^{2\times 2}_s$ consists of matrix-valued functions $\boldsymbol{U}$ with each component $U_{ij} \in L^2(D)$ and $U_{12} = U_{21}$.

Let Ω be a polygonal domain and denote a family of decompositions of $\overline{\Omega}$ by $\{\mathcal{T}_h\}_h$ that is compatible with the boundary splitting: $\Gamma = \overline{\Gamma_D} \cup \overline{\Gamma_S}$, i.e., if an element edge has a non-empty intersection with one of the sets Γ_D, and Γ_S, then the edge lies entirely in the corresponding closed set $\overline{\Gamma_D}$, or $\overline{\Gamma_S}$. For any element $K \in \mathcal{T}_h$, let $h_K = \mathrm{diam}(K)$, $h = \max\{h_K : K \in \mathcal{T}_h\}$, and $h_e = \mathrm{length}(e)$. For any edge e shared by two elements K^+ and K^-, define $\omega_e := K^+ \cup K^-$, and for any element $K \in \mathcal{T}_h$, define the patch set $\omega_K := \cup\{T \in \mathcal{T}_h,\ T \cap K \neq \emptyset\}$. Following the ideas in [54,55], we assume that, for each h and every $K \in \mathcal{T}_h$, there exist positive constants γ_1 and γ_2 such that

A1 K is star-shaped with respect to a ball of radius $\gamma_1 h_K$.

A2 The distance between any two vertices of K is greater to $\gamma_2 h_K$.

With the above two assumptions, the usual polynomial approximation properties, the trace and inverse inequalities hold true [54,56,57]. Note that A1–A2 also imply that there exists a constant $\gamma_3 > 0$ such that the following property is valid.

A3 Each $K \in \mathcal{T}_h$ can be divided by a uniformly shape regular and quasi-uniform triangulation $\mathcal{T}_h^K$ such that the mesh size of $\mathcal{T}_h^K$ is greater to $\gamma_3 h_K$ and each edge of K is a side of a triangle in $\mathcal{T}_h^K$.

Let $\mathcal{E}_h$ stand for the union of the boundaries of all the elements in $\mathcal{T}_h$, $\mathcal{E}_h^i$ is the set of all interior edges, the set of all the edges on Γ_S is denoted by $\mathcal{E}_h^S$, and $\mathcal{E}_h^0 = \mathcal{E}_h \backslash \mathcal{E}_h^S$. Let K^+ and K^- be two neighboring elements with a common edge e, and $\boldsymbol{n}^\alpha = \boldsymbol{n}|_{\partial K^\alpha}$ be the unit outward normal vector on ∂K^α with $\alpha = \pm$. For a scalar function q, set $q^\alpha = q|_{\partial K^\alpha}$ and similarly, for a vector-valued function $\boldsymbol{v}$ and a matrix-valued function $\boldsymbol{U}$, let $\boldsymbol{v}^\alpha = \boldsymbol{v}|_{\partial K^\alpha}$, $\boldsymbol{U}^\alpha = \boldsymbol{U}|_{\partial K^\alpha}$. Then define the averages $\{\cdot\}$ and the jumps $[\cdot]$, $\lfloor\cdot\rfloor$, $[\![\cdot]\!]$ on $e \in \mathcal{E}_h^i$ by

$$
\begin{aligned}
&\{q\} = \frac{1}{2}(q^+ + q^-), \qquad [q] = q^+\boldsymbol{n}^+ + q^-\boldsymbol{n}^-,\\
&\{\boldsymbol{v}\} = \frac{1}{2}(\boldsymbol{v}^+ + \boldsymbol{v}^-), \qquad [\boldsymbol{v}] = \boldsymbol{v}^+\cdot\boldsymbol{n}^+ + \boldsymbol{v}^-\cdot\boldsymbol{n}^-, \qquad \lfloor\boldsymbol{v}\rfloor = \boldsymbol{v}^+ - \boldsymbol{v}^-,\\
&[\![\boldsymbol{v}]\!] = \frac{1}{2}(\boldsymbol{v}^+\otimes\boldsymbol{n}^+ + \boldsymbol{n}^+\otimes\boldsymbol{v}^+ + \boldsymbol{v}^-\otimes\boldsymbol{n}^- + \boldsymbol{n}^-\otimes\boldsymbol{v}^-),\\
&\{\boldsymbol{U}\} = \frac{1}{2}(\boldsymbol{U}^+ + \boldsymbol{U}^-), \qquad [\boldsymbol{U}] = \boldsymbol{U}^+\boldsymbol{n}^+ + \boldsymbol{U}^-\boldsymbol{n}^-.
\end{aligned}
$$

Here, $\boldsymbol{u}\otimes\boldsymbol{v}$ is a matrix with $u_i v_j$ as its (i,j)th element. On an element edge $e \subset \Gamma$, we set

$$
\begin{aligned}
&\{q\} = q, \qquad [q] = q\boldsymbol{n},\\
&\{\boldsymbol{v}\} = \boldsymbol{v}, \qquad [\boldsymbol{v}] = \boldsymbol{v}\cdot\boldsymbol{n}, \qquad \lfloor\boldsymbol{v}\rfloor = \boldsymbol{v}, \qquad [\![\boldsymbol{v}]\!] = \frac{1}{2}(\boldsymbol{v}\otimes\boldsymbol{n} + \boldsymbol{n}\otimes\boldsymbol{v}),\\
&\{\boldsymbol{U}\} = \boldsymbol{U}, \qquad [\boldsymbol{U}] = \boldsymbol{U}\boldsymbol{n}.
\end{aligned}
$$

From the definition of the averages and jumps, by a direct manipulation, we have

$$
\sum_{K\in\mathcal{T}_h}\int_{\partial K}(\boldsymbol{U}\boldsymbol{n}_K)\cdot\boldsymbol{v}\,ds = \int_{\mathcal{E}_h^i}[\boldsymbol{U}]\cdot\{\boldsymbol{v}\}\,ds + \int_{\mathcal{E}_h}\{\boldsymbol{U}\} : [\![\boldsymbol{v}]\!]\,ds. \tag{3.1}
$$

$$
\sum_{K\in\mathcal{T}_h}\int_{\partial K}(\boldsymbol{v}\cdot\boldsymbol{n}_K)q\,ds = \int_{\mathcal{E}_h^i}[\boldsymbol{v}]\{q\}\,ds + \int_{\mathcal{E}_h}\{\boldsymbol{v}\}\cdot[q]\,ds. \tag{3.2}
$$

Let $k \geq 0$ be a non-negative integer. We introduce the following DG spaces:

$$
\begin{aligned}
\tilde{\boldsymbol{V}}^h &= \{\boldsymbol{v}^h \in [L^2(\Omega)]^2 :\ v_i^h|_K \in P_{k+1}(K)\ \forall K \in \mathcal{T}_h,\ i = 1, 2\},\\
\boldsymbol{V}^h &= \{\boldsymbol{v}^h \in \tilde{\boldsymbol{V}}^h :\ v_n^h = 0 \text{ on } \Gamma_S\},\\
\boldsymbol{W}^h &= \{\boldsymbol{\tau}^h \in [L^2(\Omega)]^{2\times 2}_s :\ \tau_{ij}^h|_K \in P_k(K)\ \forall K \in \mathcal{T}_h,\ i, j = 1, 2\},
\end{aligned}
$$

$$Q^h = \{q^h \in L_0^2(\Omega):\ q^h|_K \in P_k(K)\ \forall K \in \mathcal{T}_h\}.$$

Here, $P_k(K)$ is the set of all polynomials in K with the total degree no more than k.

We will need the lifting operators $\boldsymbol{r}_0 : \left(L^2(\mathcal{E}_h^0)\right)_s^{2\times 2} \to \boldsymbol{W}_h$, $\boldsymbol{r}_e : \left(L^2(e)\right)_s^{2\times 2} \to \boldsymbol{W}_h$, defined by

$$\int_\Omega \boldsymbol{r}_0(\boldsymbol{\phi}) : \boldsymbol{U}\,dx = -\int_{\mathcal{E}_h^0} \boldsymbol{\phi} : \{\boldsymbol{U}\}\,ds \quad \forall \boldsymbol{U} \in \boldsymbol{W}_h,\ \boldsymbol{\phi} \in \left(L^2(\mathcal{E}_h^0)\right)_s^{2\times 2}, \tag{3.3}$$

$$\int_\Omega \boldsymbol{r}_e(\boldsymbol{\phi}) : \boldsymbol{U}\,dx = -\int_e \boldsymbol{\phi} : \{\boldsymbol{U}\}\,ds \quad \forall \boldsymbol{U} \in \boldsymbol{W}_h,\ \boldsymbol{\phi} \in \left(L^2(e)\right)_s^{2\times 2}. \tag{3.4}$$

3.2. DG formulations

We now derive some DG formulations for the Stokes problem with slip boundary condition of frictional type (2.2)–(2.5). For this purpose, we rewrite the first equation in (2.2) with the help of Cauchy stress (2.1)

$$\begin{cases} \boldsymbol{T} + p\mathbf{I} = 2\,\nu\,\boldsymbol{\varepsilon}(\boldsymbol{u}) & \text{in } \Omega, \\ -\mathrm{div}\boldsymbol{T} = \boldsymbol{f} & \text{in } \Omega. \end{cases} \tag{3.5}$$

First, multiply the above equations by $(2\nu)^{-1}\boldsymbol{U}$ and $\boldsymbol{v}$, respectively, integrate on an arbitrary element K, and apply the integration by parts formula (2.10),

$$\int_K (2\nu)^{-1}(\boldsymbol{T} : \boldsymbol{U} + p\,\mathrm{tr}(\boldsymbol{U}))\,dx = -\int_K \boldsymbol{u}\cdot \mathrm{div}\boldsymbol{U}\,dx + \int_{\partial K} \boldsymbol{u}\cdot(\boldsymbol{U}\boldsymbol{n}_K)\,ds, \tag{3.6}$$

$$\int_K \boldsymbol{f}\cdot\boldsymbol{v}\,dx = \int_K \boldsymbol{T} : \boldsymbol{\varepsilon}(\boldsymbol{v})\,dx - \int_{\partial K} (\boldsymbol{T}\boldsymbol{n}_K)\cdot\boldsymbol{v}\,ds. \tag{3.7}$$

Then, we append superscript h on $\boldsymbol{T}$, $\boldsymbol{U}$, $\boldsymbol{u}$, $\boldsymbol{v}$, p, div and $\boldsymbol{\varepsilon}$ in (3.6)–(3.7), add over all the elements, and use numerical traces $\widehat{\boldsymbol{u}^h}$ and $\widehat{\boldsymbol{T}^h}$ to approximate $\boldsymbol{u}$ and $\boldsymbol{T}$ over element edges to obtain

$$\int_\Omega (2\nu)^{-1}(\boldsymbol{T}^h : \boldsymbol{U}^h + p^h\,\mathrm{tr}(\boldsymbol{U}^h))\,dx = -\int_\Omega \boldsymbol{u}^h\cdot \mathrm{div}^h\boldsymbol{U}^h\,dx + \sum_{K\in\mathcal{T}_h}\int_{\partial K} \widehat{\boldsymbol{u}^h}\cdot(\boldsymbol{U}^h\boldsymbol{n}_K)\,ds, \tag{3.8}$$

$$\int_\Omega \boldsymbol{f}\cdot\boldsymbol{v}^h\,dx = \int_\Omega \boldsymbol{T}^h : \boldsymbol{\varepsilon}^h(\boldsymbol{v}^h)\,dx - \sum_{K\in\mathcal{T}_h}\int_{\partial K} (\widehat{\boldsymbol{T}^h}\boldsymbol{n}_K)\cdot\boldsymbol{v}^h\,ds, \tag{3.9}$$

for all $(\boldsymbol{U}^h, \boldsymbol{v}^h) \in \boldsymbol{W}^h \times \boldsymbol{V}^h$. Here, $\boldsymbol{\varepsilon}^h(\boldsymbol{v})$ and $\mathrm{div}^h\boldsymbol{\tau}$ are defined by the relation $\boldsymbol{\varepsilon}^h(\boldsymbol{v}) = \boldsymbol{\varepsilon}(\boldsymbol{v})$ and $\mathrm{div}^h\boldsymbol{\tau} = \mathrm{div}\boldsymbol{\tau}$ on any element $K \in \mathcal{T}_h$.

To derive a formulation which does not rely on $\boldsymbol{T}^h$ explicitly, using (2.10) and (3.1), we have from (3.8) and (3.9) that

$$\begin{aligned} \int_\Omega (2\nu)^{-1}(\boldsymbol{T}^h : \boldsymbol{U}^h + p^h\,\mathrm{tr}(\boldsymbol{U}^h))\,dx &= \int_\Omega \boldsymbol{\varepsilon}^h(\boldsymbol{u}^h) : \boldsymbol{U}^h\,dx + \int_{\mathcal{E}_h^i} \{\widehat{\boldsymbol{u}^h} - \boldsymbol{u}^h\}\cdot[\boldsymbol{U}^h]\,ds \\ &\quad + \int_{\mathcal{E}_h} [\![\widehat{\boldsymbol{u}^h} - \boldsymbol{u}^h]\!] : \{\boldsymbol{U}^h\}\,ds, \end{aligned} \tag{3.10}$$

$$\begin{aligned} \int_\Omega \boldsymbol{f}\cdot\boldsymbol{v}^h\,dx &= \int_\Omega \boldsymbol{T}^h : \boldsymbol{\varepsilon}^h(\boldsymbol{v}^h)\,dx - \int_{\mathcal{E}_h^i} [\widehat{\boldsymbol{T}^h}]\cdot\{\boldsymbol{v}^h\}\,ds \\ &\quad - \int_{\mathcal{E}_h} [\![\boldsymbol{v}^h]\!] : \{\widehat{\boldsymbol{T}^h}\}\,ds. \end{aligned} \tag{3.11}$$

Note that, by the definition of the lifting operator $\boldsymbol{r}_0$, we have from (3.10) that

$$\boldsymbol{T}^h = 2\nu\boldsymbol{\varepsilon}^h(\boldsymbol{u}^h) - p^h\mathbf{I} + 2\nu\boldsymbol{r}_0([\![\boldsymbol{u}^h]\!]).$$

Choosing $\boldsymbol{U}^h = 2\nu\boldsymbol{\varepsilon}^h(\boldsymbol{v}^h)$ in (3.10), we get

$$\begin{aligned} \int_\Omega \boldsymbol{T}^h : \boldsymbol{\varepsilon}^h(\boldsymbol{v}^h) + p^h\,\mathrm{tr}(\boldsymbol{\varepsilon}^h(\boldsymbol{v}^h))\,dx &= 2\nu\Big(\int_\Omega \boldsymbol{\varepsilon}^h(\boldsymbol{u}^h) : \boldsymbol{\varepsilon}^h(\boldsymbol{v}^h)\,dx + \int_{\mathcal{E}_h^i} \{\widehat{\boldsymbol{u}^h} - \boldsymbol{u}^h\}\cdot[\boldsymbol{\varepsilon}^h(\boldsymbol{v}^h)]\,ds \\ &\quad + \int_{\mathcal{E}_h} [\![\widehat{\boldsymbol{u}^h} - \boldsymbol{u}^h]\!] : \{\boldsymbol{\varepsilon}^h(\boldsymbol{v}^h)\}\,ds\Big). \end{aligned}$$

Table 1
Choices of $\widehat{\boldsymbol{T}^h}$ on $\mathcal{E}_h^0$ for different DG schemes.

Methods	Numerical flux $\widehat{\boldsymbol{T}^h}$ on $\mathcal{E}_h^0$
IP [58]	$\{2\nu\boldsymbol{\varepsilon}^h(\boldsymbol{u}^h)-p^h\mathbf{I}\}-2\nu\eta_e h_e^{-1}[\![\boldsymbol{u}^h]\!]$
Bassi et al. [33]	$\{2\nu\boldsymbol{\varepsilon}^h(\boldsymbol{u}^h)-p^h\mathbf{I}\}+\eta_e\{2\nu\boldsymbol{r}_e([\![\boldsymbol{u}^h]\!])\}$
Brezzi et al. [59]	$\{2\nu\boldsymbol{\varepsilon}^h(\boldsymbol{u}^h)-p^h\mathbf{I}\}+\{2\nu\boldsymbol{r}_0([\![\boldsymbol{u}^h]\!])\}+\eta_e\{2\nu\boldsymbol{r}_e([\![\boldsymbol{u}^h]\!])\}$
Local DG [60]	$\{2\nu\boldsymbol{\varepsilon}^h(\boldsymbol{u}^h)-p^h\mathbf{I}\}+\{2\nu\boldsymbol{r}_0([\![\boldsymbol{u}^h]\!])\}-2\nu\eta_e h_e^{-1}[\![\boldsymbol{u}^h]\!]$

Combination of this equation and (3.11) yields

$$2\nu\left(\int_\Omega \boldsymbol{\varepsilon}^h(\boldsymbol{u}^h):\boldsymbol{\varepsilon}^h(\boldsymbol{v}^h)\,dx+\int_{\mathcal{E}_h^i}\{\widehat{\boldsymbol{u}^h}-\boldsymbol{u}^h\}\cdot[\boldsymbol{\varepsilon}^h(\boldsymbol{v}^h)]\,ds+\int_{\mathcal{E}_h}[\![\widehat{\boldsymbol{u}^h}-\boldsymbol{u}^h]\!]:\{\boldsymbol{\varepsilon}^h(\boldsymbol{v}^h)\}\,ds\right)$$
$$-\int_\Omega p^h\,\mathrm{div}^h\boldsymbol{v}^h\,dx-\int_{\mathcal{E}_h^i}[\widehat{\boldsymbol{T}^h}]\cdot\{\boldsymbol{v}^h\}\,ds-\int_{\mathcal{E}_h}[\![\boldsymbol{v}^h]\!]:\{\widehat{\boldsymbol{T}^h}\}\,ds=\int_\Omega \boldsymbol{f}\cdot\boldsymbol{v}^h\,dx. \tag{3.12}$$

The numerical traces $\widehat{\boldsymbol{T}^h}$ and $\widehat{\boldsymbol{u}^h}$ will be selected to guarantee consistency and stability of the scheme. We introduce four consistent and stable DG methods. For all the DG methods in this paper, we let $\widehat{\boldsymbol{u}^h}$ and $\widehat{\boldsymbol{T}^h}$ satisfy the non-leak and slip boundary conditions (2.4)–(2.5), i.e.,

$$\left.\begin{array}{l}\widehat{u_n^h}=0,\quad \widehat{\boldsymbol{u}_\tau^h}=\boldsymbol{u}_\tau^h\\ |\widehat{\boldsymbol{T}_\tau^h}|\le g,\quad \widehat{\boldsymbol{T}_\tau^h}\cdot\widehat{\boldsymbol{u}_\tau^h}+g|\widehat{\boldsymbol{u}_\tau^h}|=0\end{array}\right\}\text{ on }\Gamma_S. \tag{3.13}$$

In addition, for all the following DG methods, we choose numerical fluxes $\widehat{\boldsymbol{u}^h}$ as

$$\widehat{\boldsymbol{u}^h}=\{\boldsymbol{u}^h\}\quad\text{on }\mathcal{E}_h^i,\qquad \widehat{\boldsymbol{u}^h}=\boldsymbol{0}\quad\text{on }\Gamma_D. \tag{3.14}$$

Let

$$\widehat{\boldsymbol{T}^h}=\{2\nu\boldsymbol{\varepsilon}^h(\boldsymbol{u}^h)-p^h\mathbf{I}\}-2\nu\eta_e h_e^{-1}[\![\boldsymbol{u}^h]\!]\quad\text{on }\mathcal{E}_h^0,$$

where $\eta_e>0$ is the penalty parameter on $e\in\mathcal{E}_h^0$. Then we obtain from (3.12) that

$$A_h^{(1)}(\boldsymbol{u}^h,\boldsymbol{v}^h)+B_h(\boldsymbol{v}^h,p^h)=\int_\Omega \boldsymbol{f}\cdot\boldsymbol{v}^h\,dx+\int_{\Gamma_S}\widehat{\boldsymbol{T}_\tau^h}\cdot\boldsymbol{v}_\tau^h\,ds, \tag{3.15}$$

where

$$A_h^{(1)}(\boldsymbol{u}^h,\boldsymbol{v}^h):=2\nu\Big(\int_\Omega \boldsymbol{\varepsilon}^h(\boldsymbol{u}^h):\boldsymbol{\varepsilon}^h(\boldsymbol{v}^h)\,dx-\int_{\mathcal{E}_h^0}[\![\boldsymbol{u}^h]\!]:\{\boldsymbol{\varepsilon}^h(\boldsymbol{v}^h)\}\,ds$$
$$-\int_{\mathcal{E}_h^0}[\![\boldsymbol{v}^h]\!]:\{\boldsymbol{\varepsilon}^h(\boldsymbol{u}^h)\}\,ds+\int_{\mathcal{E}_h^0}\eta_e h_e^{-1}[\![\boldsymbol{u}^h]\!]:[\![\boldsymbol{v}^h]\!]\,ds\Big). \tag{3.16}$$

and

$$B_h(\boldsymbol{v}^h,p^h):=-\int_\Omega p^h\,\mathrm{div}^h\boldsymbol{v}^h\,dx+\int_{\mathcal{E}_h^0}[\boldsymbol{v}^h]\{p^h\}\,ds. \tag{3.17}$$

From the divergence free condition $\mathrm{div}\boldsymbol{u}=0$, we can use a similar argument to derive

$$B_h(\boldsymbol{u}^h,q^h)=0. \tag{3.18}$$

In (3.15), set $\boldsymbol{v}^h=\boldsymbol{w}^h-\boldsymbol{u}^h$ with $\boldsymbol{w}^h\in\boldsymbol{V}^h$. For all $(\boldsymbol{w}^h,q^h)\in\boldsymbol{V}^h\times Q^h$, using (3.13), we can derive

$$A_h^{(1)}(\boldsymbol{u}^h,\boldsymbol{w}^h-\boldsymbol{u}^h)+B_h(\boldsymbol{w}^h-\boldsymbol{u}^h,p^h)+j(\boldsymbol{w}_\tau^h)-j(\boldsymbol{u}_\tau^h)\ge(\boldsymbol{f},\boldsymbol{w}^h-\boldsymbol{u}^h)_V, \tag{3.19}$$
$$B_h(\boldsymbol{u}^h,q^h)=0, \tag{3.20}$$

which is the interior penalty (IP) DG scheme [58].

Choosing different numerical fluxes, we derive four DG schemes, see Table 1 for the choices of $\widehat{\boldsymbol{T}^h}$ and Table 2 for the different bilinear forms A_h.

In Table 2, the short notation is defined as follows.

$$\tilde{a}:=2\nu\Big(\int_\Omega \boldsymbol{\varepsilon}^h(\boldsymbol{u}^h):\boldsymbol{\varepsilon}^h(\boldsymbol{v}^h)\,dx-\int_{\mathcal{E}_h^0}[\![\boldsymbol{u}^h]\!]:\{\boldsymbol{\varepsilon}^h(\boldsymbol{v}^h)\}\,ds-\int_{\mathcal{E}_h^0}[\![\boldsymbol{v}^h]\!]:\{\boldsymbol{\varepsilon}^h(\boldsymbol{u}^h)\}\,ds\Big),$$

Table 2
DG formulations for the bilinear form A_h.

Methods	Bilinear forms
IP [58]	$A_h^{(1)} = \tilde{a} + \beta^\alpha$
Bassi et al. [33]	$A_h^{(2)} = \tilde{a} + \beta^r$
Brezzi et al. [59]	$A_h^{(3)} = \tilde{a} + \tilde{r} + \beta^r$
Local DG [60]	$A_h^{(4)} = \tilde{a} + \tilde{r} + \beta^\alpha$

$$\beta^\alpha := 2\nu \int_{\mathcal{E}_h^0} \eta_e h_e^{-1} [\![\boldsymbol{u}^h]\!] : [\![\boldsymbol{v}^h]\!] \, ds,$$

$$\beta^r := 2\nu \sum_{e \in \mathcal{E}_h^0} \int_\Omega \eta_e \boldsymbol{r}_e([\![\boldsymbol{u}^h]\!]) : \boldsymbol{r}_e([\![\boldsymbol{v}^h]\!]) \, dx$$

$$\tilde{r} := \int_\Omega \boldsymbol{r}_0([\![\boldsymbol{v}^h]\!]) : \boldsymbol{r}_0([\![\boldsymbol{u}^h]\!]) \, dx$$

Let $A_h(\boldsymbol{u}^h, \boldsymbol{v}^h)$ be one of the bilinear forms $A_h^{(j)}(\boldsymbol{u}^h, \boldsymbol{v}^h)$ with $j = 1, \ldots, 4$. Then a DG method for the problem (2.12) is: Find $(\boldsymbol{u}^h, p^h) \in \boldsymbol{V}^h \times Q^h$ such that

$$A_h(\boldsymbol{u}^h, \boldsymbol{v}^h - \boldsymbol{u}^h) + B_h(\boldsymbol{v}^h - \boldsymbol{u}^h, p^h) + j(\boldsymbol{v}_\tau^h) - j(\boldsymbol{u}_\tau^h) \geq (\boldsymbol{f}, \boldsymbol{v}^h - \boldsymbol{u}^h), \tag{3.21}$$

$$B_h(\boldsymbol{u}^h, q^h) = 0, \tag{3.22}$$

for all $(\boldsymbol{v}^h, q^h) \in \boldsymbol{V}^h \times Q^h$. The well-posedness of the above DG schemes can be proved, and a priori error analysis is given in [43,45].

3.3. Lagrangian multiplier in the DG formulation

By similar argument for the continuous problem [25,53], there exists a Lagrange multiplier $\boldsymbol{\lambda}_\tau^h \in [L^\infty(\Gamma_S)]^2$ such that

$$A_h(\boldsymbol{u}^h, \boldsymbol{v}^h) + B_h(\boldsymbol{v}^h, p^h) = (\boldsymbol{f}, \boldsymbol{v}^h) - \int_{\Gamma_S} g \, \boldsymbol{\lambda}_\tau^h \cdot \boldsymbol{v}_\tau^h \, ds \qquad \forall \, \boldsymbol{v}^h \in \boldsymbol{V}^h, \tag{3.23}$$

$$B_h(\boldsymbol{u}^h, q^h) = 0 \qquad \forall \, q^h \in Q^h, \tag{3.24}$$

$$|\boldsymbol{\lambda}_\tau^h| \leq 1, \quad \boldsymbol{\lambda}_\tau^h \cdot \boldsymbol{u}_\tau^h = |\boldsymbol{u}_\tau^h| \quad \text{a.e. on } \Gamma_S. \tag{3.25}$$

Let

$$\ell^h(\boldsymbol{v}^h) = (\boldsymbol{f}, \boldsymbol{v}^h) - \int_{\Gamma_S} g \, \boldsymbol{\lambda}_\tau^h \cdot \boldsymbol{v}_\tau^h \, ds,$$

we get

$$A_h(\boldsymbol{u}^h, \boldsymbol{v}^h) + B_h(\boldsymbol{v}^h, p^h) = \ell^h(\boldsymbol{v}^h). \tag{3.26}$$

For any $\boldsymbol{u}, \boldsymbol{v} \in \boldsymbol{V}$, we know that $[\![\boldsymbol{u}]\!] = 0$, $[\![\boldsymbol{v}]\!] = 0$, $[\boldsymbol{u}] = 0$, and $[\boldsymbol{v}] = 0$ on $e \in \mathcal{E}_h^0$. Then we have from (2.14) that

$$A_h(\boldsymbol{u}, \boldsymbol{v}) + B_h(\boldsymbol{v}, p) = a(\boldsymbol{u}, \boldsymbol{v}) + b(\boldsymbol{v}, p) = \ell(\boldsymbol{v}) \qquad \forall \, \boldsymbol{v} \in \boldsymbol{V}, \tag{3.27}$$

$$B_h(\boldsymbol{u}, q) = b(\boldsymbol{u}, q) = 0 \qquad \forall \, q \in Q. \tag{3.28}$$

Obviously, $\boldsymbol{u}^h$ and p^h are also the DG approximation of the solution $\boldsymbol{z} \in \boldsymbol{V}$ and $y \in Q$ of the problem:

$$a(\boldsymbol{z}, \boldsymbol{v}) + b(\boldsymbol{v}, y) = \ell^h(\boldsymbol{v}) \qquad \forall \, \boldsymbol{v} \in \boldsymbol{V}, \tag{3.29}$$

$$b(\boldsymbol{z}, q) = 0 \qquad \forall \, q \in Q. \tag{3.30}$$

From (3.27)–(3.30), we have

$$a(\boldsymbol{u} - \boldsymbol{z}, \boldsymbol{v}) + b(\boldsymbol{v}, p - y) = \int_{\Gamma_S} g \, (\boldsymbol{\lambda}_\tau^h - \boldsymbol{\lambda}_\tau) \cdot \boldsymbol{v}_\tau ds, \tag{3.31}$$

$$b(\boldsymbol{u} - \boldsymbol{z}, q) = 0. \tag{3.32}$$

Recall (2.16), we have

$$|\boldsymbol{\lambda}_\tau - \boldsymbol{\lambda}_\tau^h|_{*,\Gamma_S} \lesssim \|\boldsymbol{u} - \boldsymbol{z}\|_{h,V} + \|p - y\|. \tag{3.33}$$

In addition, we have the following lemma about the consistency of the DG schemes.

Lemma 3.1. *Assume $\boldsymbol{u} \in \boldsymbol{V}$ and $p \in Q$ for the solution of (2.12), and $\boldsymbol{z} \in \boldsymbol{V}$ and $y \in Q$ for the solution of (3.29)–(3.30). Then for the DG methods $A_h(\boldsymbol{w}, \boldsymbol{v}) = A_h^{(j)}(\boldsymbol{w}, \boldsymbol{v})$ with $j = 1, \dots, 4$, we have*

$$A_h(\boldsymbol{u}, \boldsymbol{v}^h) + B_h(\boldsymbol{v}^h, p) = \ell(\boldsymbol{v}^h) \quad \forall \boldsymbol{v}^h \in \boldsymbol{V}^h, \tag{3.34}$$

$$A_h(\boldsymbol{z}, \boldsymbol{v}^h) + B_h(\boldsymbol{v}^h, y) = \ell^h(\boldsymbol{v}^h) \quad \forall \boldsymbol{v}^h \in \boldsymbol{V}^h. \tag{3.35}$$

Proof. Since $-\mathrm{div}\boldsymbol{T} = \boldsymbol{f} \in [L^2(\Omega)]^2$, $\boldsymbol{T} \in H(\mathrm{div}, \Omega; \mathbb{S}^d)$ and $[\boldsymbol{T}] = 0$ on any interior edge e. For $\boldsymbol{u} \in \boldsymbol{V}$, $[\![\boldsymbol{u}]\!] = \boldsymbol{0}$ and $\{\boldsymbol{u}\} = \boldsymbol{u}$ on any interior edge e. Using (2.1), we obtain, for any $\boldsymbol{v}^h \in \boldsymbol{V}^h$,

$$\begin{aligned}
A_h(\boldsymbol{u}, \boldsymbol{v}^h) + B_h(\boldsymbol{v}^h, p) =& 2\nu \left(\int_\Omega \boldsymbol{\varepsilon}(\boldsymbol{u}) : \boldsymbol{\varepsilon}^h(\boldsymbol{v}^h)\, dx - \int_{\mathcal{E}_h^0} [\![\boldsymbol{v}^h]\!] : \{\boldsymbol{\varepsilon}(\boldsymbol{u})\}\, ds \right) \\
& - \int_\Omega p\, \mathrm{div}^h(\boldsymbol{v}^h)\, dx + \int_{\mathcal{E}_h^0} [\boldsymbol{v}^h]\{p\}\, ds \\
=& \sum_{K \in \mathcal{T}_h} \int_K \boldsymbol{T} : \boldsymbol{\varepsilon}^h(\boldsymbol{v}^h)\, dx - \int_{\mathcal{E}_h^0} [\![\boldsymbol{v}^h]\!] : \{\boldsymbol{T}\}\, ds.
\end{aligned}$$

By (2.10), (3.1) and noting that $[\boldsymbol{T}] = \boldsymbol{0}$ on $\mathcal{E}_h^i$, we get

$$\begin{aligned}
\sum_{K \in \mathcal{T}_h} \int_K \boldsymbol{T} : \boldsymbol{\varepsilon}^h(\boldsymbol{v}^h)\, dx &= \sum_{K \in \mathcal{T}_h} \int_K -\mathrm{div}\boldsymbol{T} \cdot \boldsymbol{v}^h\, dx + \sum_{K \in \mathcal{T}_h} \int_{\partial K} (\boldsymbol{T}\boldsymbol{n}_K) \cdot \boldsymbol{v}^h\, ds \\
&= \sum_{K \in \mathcal{T}_h} \int_K \boldsymbol{f} \cdot \boldsymbol{v}^h\, dx + \int_{\mathcal{E}_h} [\![\boldsymbol{v}^h]\!] : \{\boldsymbol{T}\}\, ds.
\end{aligned}$$

Then

$$\begin{aligned}
A_h(\boldsymbol{u}, \boldsymbol{v}^h) + B_h(\boldsymbol{v}^h, p) &= \int_\Omega \boldsymbol{f} \cdot \boldsymbol{v}^h\, dx + \int_{\Gamma_S} (\boldsymbol{T}\boldsymbol{n}) \cdot \boldsymbol{v}^h\, ds \\
&= \int_\Omega \boldsymbol{f} \cdot \boldsymbol{v}^h\, dx + \int_{\Gamma_S} \boldsymbol{T}_\tau \cdot \boldsymbol{v}_\tau^h\, ds \\
&= \int_\Omega \boldsymbol{f} \cdot \boldsymbol{v}^h\, dx - \int_{\Gamma_S} g\, \boldsymbol{\lambda}_\tau \cdot \boldsymbol{v}_\tau^h\, ds.
\end{aligned}$$

The last equality is obtained by (2.15).

The second equation (3.35) can be proved by similar argument. ■

By (3.26), (3.34) and (3.35), we get

$$A_h(\boldsymbol{u} - \boldsymbol{u}^h, \boldsymbol{v}^h) + B_h(\boldsymbol{v}^h, p - p^h) = \int_{\Gamma_S} g\, (\boldsymbol{\lambda}_\tau^h - \boldsymbol{\lambda}_\tau) \cdot \boldsymbol{v}_\tau^h\, ds, \tag{3.36}$$

$$A_h(\boldsymbol{z} - \boldsymbol{u}^h, \boldsymbol{v}^h) + B_h(\boldsymbol{v}^h, y - p^h) = 0 \tag{3.37}$$

for any $\boldsymbol{v}^h \in \boldsymbol{V}^h$.

4. A posteriori error analysis

4.1. Divergence free solution constructed from DG solution

To derive reliable and efficient a posteriori error estimators, we introduce a divergence free solution constructed from the DG solution $\boldsymbol{u}^h \in \boldsymbol{V}^h$. We present a post-processing operator $\mathbb{P}$, from the space of totally discontinuous velocities to the space of velocities that have continuous components, such that $\mathbb{P}\boldsymbol{u}^h$ is divergence free.

For $k \in \mathbb{N}$, let us define the spaces

- $B_k(\partial K) = \{v \in C^0(\partial K) : v|_e \in P_k(e) \quad \forall \text{ edge } e \subset \partial K\}$,
- $\mathbf{G}_k(K) = \nabla(P_{k+1}(K)) \subseteq [P_k(K)]^2$,
- $\mathbf{G}_k^\perp(K)$, the $L^2(K)$-orthogonal complement of $\mathbf{G}_k(K)$ in $[P_k(K)]^2$.

On each element $K \in \mathcal{T}_h$, we define the following local space

$$\boldsymbol{U}_K^h = \Big\{ \boldsymbol{v} \in [H^1(K)]^2 : \ \boldsymbol{v}|_{\partial K} \in [B_{k+1}(\partial K)]^2, \ \operatorname{div} \boldsymbol{v} \in P_k(K), \\ - \operatorname{div}(2\nu\boldsymbol{\varepsilon}(\boldsymbol{v})) - \nabla s \in \mathbf{G}_{k-1}^{\perp}(K) \text{ for some } s \in L^2(K) \Big\}.$$

Then we define the global space as

$$\boldsymbol{U}^h = \{ \boldsymbol{v} \in \boldsymbol{V} \quad \text{s.t} \quad \boldsymbol{v}|_K \in \boldsymbol{U}_K^h \quad \text{for each } K \in \mathcal{T}_h \}.$$

For the DG solution $\boldsymbol{u}^h \in \boldsymbol{V}^h$, we define the operator $\mathbb{P} : \boldsymbol{V}^h \to \boldsymbol{U}^h$ by

$$(\mathbb{P}\boldsymbol{u}^h)|_K = \mathbb{P}_K(\boldsymbol{u}^h|_K) \quad \text{for each } K \in \mathcal{T}_h.$$

Let $\{\boldsymbol{x}_i^e\}_{i=1}^{k+2} \subset e$ be the set of Gauss–Lobatto points on every edge $e \subset \partial K$. We define the local operator $\mathbb{P}_K : [P_{k+1}(K)]^2 \to \boldsymbol{U}_K^h$ as follows:

$$\mathbb{P}_K \boldsymbol{u}^h(\boldsymbol{x}_i^e) = \widehat{\boldsymbol{u}^h}(\boldsymbol{x}_i^e) \quad 1 \le i \le k+2, \ e \subset \partial K, \tag{4.1}$$

$$\int_K (\mathbb{P}_K \boldsymbol{u}^h) \cdot \boldsymbol{g}_{k-1} \, d\boldsymbol{x} = \int_K \boldsymbol{u}^h \cdot \boldsymbol{g}_{k-1} \, d\boldsymbol{x} \quad \forall \boldsymbol{g}_{k-1} \in \mathbf{G}_{k-1}(K), \tag{4.2}$$

$$\int_K (\mathbb{P}_K \boldsymbol{u}^h) \cdot \boldsymbol{g}_{k-1}^{\perp} \, d\boldsymbol{x} = \int_K \boldsymbol{u}^h \cdot \boldsymbol{g}_{k-1}^{\perp} \, d\boldsymbol{x} \quad \forall \boldsymbol{g}_{k-1}^{\perp} \in \mathbf{G}_{k-1}^{\perp}(K). \tag{4.3}$$

By (4.1), we have

$$\mathbb{P}_K \boldsymbol{u}^h = \widehat{\boldsymbol{u}^h} \quad \text{on } \partial K. \tag{4.4}$$

Lemma 4.1. *The conditions (4.1)–(4.3) uniquely determine $\mathbb{P}_K \boldsymbol{u}^h$.*

Proof. We only need to show that if $\boldsymbol{v} \in \boldsymbol{U}_K^h$ satisfies

$$\boldsymbol{v}(\boldsymbol{x}_i^e) = 0 \quad 1 \le i \le k+2, \ e \subset \partial K, \tag{4.5}$$

$$\int_K \boldsymbol{v} \cdot \boldsymbol{g}_{k-1} \, d\boldsymbol{x} = 0 \quad \forall \boldsymbol{g}_{k-1} \in \mathbf{G}_{k-1}(K), \tag{4.6}$$

$$\int_K \boldsymbol{v} \cdot \boldsymbol{g}_{k-1}^{\perp} \, d\boldsymbol{x} = 0 \quad \forall \boldsymbol{g}_{k-1}^{\perp} \in \mathbf{G}_{k-1}^{\perp}(K), \tag{4.7}$$

then $\boldsymbol{v}$ vanishes on K.

The first condition implies that $\boldsymbol{v}|_{\partial K} = \mathbf{0}$. Moreover

$$\int_K (\operatorname{div} \boldsymbol{v})^2 \, d\boldsymbol{x} = -\int_K \boldsymbol{v} \cdot \nabla(\operatorname{div} \boldsymbol{v}) \, d\boldsymbol{x} + \int_{\partial K} \boldsymbol{v} \cdot \boldsymbol{n} \operatorname{div} \boldsymbol{v} \, ds = 0.$$

The first term on the right-hand side is zero because $\operatorname{div} \boldsymbol{v} \in P_k(K)$. Therefore, we get $\operatorname{div} \boldsymbol{v} = 0$. Moreover, there exist functions $q \in L^2(K)$ and $\boldsymbol{g}_{k-1}^{\perp} \in \mathbf{G}_{k-1}^{\perp}(K)$ such that

$$-\operatorname{div}(\boldsymbol{\varepsilon}(\boldsymbol{v})) = \nabla q + \boldsymbol{g}_{k-1}^{\perp}.$$

Then

$$\begin{aligned} \int_K \boldsymbol{\varepsilon}(\boldsymbol{v}) : \boldsymbol{\varepsilon}(\boldsymbol{v}) \, d\boldsymbol{x} &= -\int_K \operatorname{div}(\boldsymbol{\varepsilon}(\boldsymbol{v})) \cdot \boldsymbol{v} \, d\boldsymbol{x} \\ &= \int_K \nabla q \cdot \boldsymbol{v} \, d\boldsymbol{x} + \int_K \boldsymbol{g}_{k-1}^{\perp} \cdot \boldsymbol{v} \, d\boldsymbol{x} \\ &= -\int_K q \operatorname{div} \boldsymbol{v} \, d\boldsymbol{x} \\ &= 0. \end{aligned}$$

Thus, $\boldsymbol{\varepsilon}(\boldsymbol{v}) = \mathbf{0}$. By Korn's inequality, we have $\boldsymbol{v} = \mathbf{0}$, which completes the proof. ■

Lemma 4.2. *$\mathbb{P}\boldsymbol{u}^h$ is divergence free.*

Proof. We first observe that div $(\mathbb{P}\boldsymbol{u}^h)|_K \in P_k(K)$ for each $K \in \mathcal{T}_h$ and

$$\begin{aligned}\int_\Omega \operatorname{div} \mathbb{P}\boldsymbol{u}^h \, d\boldsymbol{x} = \int_\Gamma \mathbb{P}\boldsymbol{u}^h \cdot \boldsymbol{n} \, ds = \int_\Gamma \widehat{\boldsymbol{u}^h} \cdot \boldsymbol{n} \, ds \\ = \int_{\Gamma_D} \widehat{\boldsymbol{u}^h} \cdot \boldsymbol{n} \, ds + \int_{\Gamma_S} \widehat{\boldsymbol{u}^h} \cdot \boldsymbol{n} \, ds \\ = 0,\end{aligned}$$

which implies that div $\mathbb{P}\boldsymbol{u}^h \in Q_h$. Here, we use the definition of the numerical flux $\widehat{\boldsymbol{u}^h}$, see (3.13)–(3.14).

Next, let $q_h \in Q_h$, we obtain

$$\begin{aligned}\int_\Omega \operatorname{div} \mathbb{P}\boldsymbol{u}^h \, q_h \, d\boldsymbol{x} &= \sum_{K\in\mathcal{T}_h} \left(\int_{\partial K} (\mathbb{P}_K \boldsymbol{u}^h) \cdot \boldsymbol{n} \, q_h \, ds - \int_K (\mathbb{P}_K \boldsymbol{u}^h) \cdot \nabla q_h \, d\boldsymbol{x} \right) \\ &= \sum_{K\in\mathcal{T}_h} \left(\int_{\partial K} \widehat{\boldsymbol{u}^h} \cdot \boldsymbol{n} \, q_h \, ds - \int_K \boldsymbol{u}^h \cdot \nabla q_h \, d\boldsymbol{x} \right) \\ &= 0.\end{aligned}$$

The last equality is due to (3.18). Thus, we have div $\mathbb{P}\boldsymbol{u}^h = 0$ in Ω. ■

Lemma 4.3. *There exists a positive constant C independent of h such that*

$$|\mathbb{P}\boldsymbol{u}^h - \boldsymbol{u}^h|_{1,h} \le C \left(\sum_{e\in\mathcal{E}_h} h_e^{-1} \| \lfloor \boldsymbol{u}^h \rfloor \|_e^2 \right)^{\frac{1}{2}}, \tag{4.8}$$

where the broken semi-norm is defined by $|\cdot|_{1,h}^2 = \sum_{K\in\mathcal{T}_h} |\cdot|_{1,K}^2$.

Proof. Setting $\boldsymbol{w}^h = \mathbb{P}\boldsymbol{u}^h - \boldsymbol{u}^h$. From (4.1)–(4.3), we know

$$\boldsymbol{w}^h = \widehat{\boldsymbol{u}^h} - \boldsymbol{u}^h \quad \text{on } \partial K, \tag{4.9}$$

$$\int_K \boldsymbol{w}^h \cdot \boldsymbol{g}_{k-1} \, d\boldsymbol{x} = 0 \quad \forall \boldsymbol{g}_{k-1} \in \mathbf{G}_{k-1}(K), \tag{4.10}$$

$$\int_K \boldsymbol{w}^h \cdot \boldsymbol{g}_{k-1}^\perp \, d\boldsymbol{x} = 0 \quad \forall \boldsymbol{g}_{k-1}^\perp \in \mathbf{G}_{k-1}^\perp(K). \tag{4.11}$$

Denote the neighboring element of $K \in \mathcal{T}_h$ sharing the edge $e \subset \partial K$ by K_e^n. Then,

$$\boldsymbol{w}^h = \frac{1}{2}(\boldsymbol{u}^h|_{K_e^n} - \boldsymbol{u}^h|_K). \tag{4.12}$$

Let us define the space

$$\begin{aligned}V(\widetilde{K}) = \Big\{ \widetilde{\boldsymbol{v}} \in \boldsymbol{U}_{\widetilde{K}}^h : \int_{\widetilde{K}} \widetilde{\boldsymbol{v}} \cdot \widetilde{\boldsymbol{g}}_{k-1} \, d\widetilde{\boldsymbol{x}} = 0 \quad \forall \widetilde{\boldsymbol{g}}_{k-1} \in \mathbf{G}_{k-1}(\widetilde{K}), \\ \int_{\widetilde{K}} \widetilde{\boldsymbol{v}} \cdot \widetilde{\boldsymbol{g}}_{k-1}^\perp \, d\widetilde{\boldsymbol{x}} = 0 \quad \forall \widetilde{\boldsymbol{g}}_{k-1}^\perp \in \mathbf{G}_{k-1}^\perp(\widetilde{K}) \Big\},\end{aligned}$$

where $\widetilde{K}$ is the reference element. Note that for $\widetilde{\boldsymbol{v}} \in V(\widetilde{K})$, if $\widetilde{\boldsymbol{v}} = \mathbf{0}$ on $\partial\widetilde{K}$, then $\widetilde{\boldsymbol{v}} = \mathbf{0}$ on $\widetilde{K}$. Thus, $\|\cdot\|_{0,\partial\widetilde{K}}$ is a norm for the space $V(\widetilde{K})$. This follows from the proof of Lemma 4.1. By a scaling argument, we have

$$\|\boldsymbol{w}^h\|_{0,K} \le Ch_K \|\widetilde{\boldsymbol{w}^h}\|_{0,\widetilde{K}} \le Ch_K \|\widetilde{\boldsymbol{w}^h}\|_{0,\partial\widetilde{K}} \le Ch_K^{\frac{1}{2}} \|\boldsymbol{w}^h\|_{0,\partial K} \le Ch_K^{\frac{1}{2}} \| \lfloor \boldsymbol{u}^h \rfloor \|_{0,\partial K}.$$

By the inverse inequality, we can derive that

$$\sum_{K\in\mathcal{T}_h} |\mathbb{P}\boldsymbol{u}^h - \boldsymbol{u}^h|_{1,K}^2 \le C \sum_{e\in\mathcal{E}_h} h_e^{-1} \| \lfloor \boldsymbol{u}^h \rfloor \|_e^2,$$

i.e., (4.8) holds. ■

4.2. Reliable residual type error estimators

Setting $\bar{\boldsymbol{T}}^h = 2\nu\boldsymbol{\varepsilon}(\boldsymbol{u}^h) - p^h\boldsymbol{I}$, we define the local residual

$$\boldsymbol{R}_K = \boldsymbol{f} + \operatorname{div}(2\nu\boldsymbol{\varepsilon}(\boldsymbol{u}^h)) - \nabla p_h \quad \text{for each } K \in \mathcal{T}_h,$$

$$\boldsymbol{R}_e = [\bar{\boldsymbol{T}}^h] \quad \text{on } \mathcal{E}_h^i, \qquad \boldsymbol{R}_e = \bar{\boldsymbol{T}}_\tau^h + g\boldsymbol{\lambda}_\tau^h \quad \text{on } \mathcal{E}_h^S,$$

and the global error estimator

$$\eta^2 = \sum_{K\in\mathcal{T}_h} h_K^2 \|\boldsymbol{R}_K\|_K^2 + \sum_{e\in\mathcal{E}_h^i\cup\mathcal{E}_h^S} h_e\|\boldsymbol{R}_e\|_e^2 + |\boldsymbol{u}^h|_*^2,$$

where

$$|\boldsymbol{u}^h|_*^2 := \sum_{e\in\mathcal{E}_h} h_e^{-1}\|\lfloor \boldsymbol{u}^h \rfloor\|_e^2.$$

Theorem 4.4. *Let $(\boldsymbol{u}, p, \boldsymbol{\lambda}_\tau)$ be the solution of (2.13), and let $(\boldsymbol{u}^h, p^h, \boldsymbol{\lambda}_\tau^h)$ be the solution of (3.23)–(3.25). Then*

$$\|\boldsymbol{u}-\boldsymbol{u}^h\|_{h,V} + \|p-p^h\| + |\boldsymbol{\lambda}_\tau - \boldsymbol{\lambda}_\tau^h|_{*,\Gamma_S} \lesssim \eta. \tag{4.13}$$

To prove Theorem 4.4, we need the following two lemmas. In the proof of Lemmas 4.5–4.6, we only consider the IPDG scheme (3.16), and similar argument can be applied to the other three DG schemes.

Lemma 4.5.

$$\|\boldsymbol{u}-\boldsymbol{u}^h\|_{h,V} + \|p-p^h\| + |\boldsymbol{\lambda}_\tau - \boldsymbol{\lambda}_\tau^h|_{*,\Gamma_S} \lesssim \eta + \|\boldsymbol{z}-\boldsymbol{u}^h\|_{h,V} + \|y-p^h\|.$$

Proof. Since $p-p^h \in L_0^2(\Omega)$, there exists a $\boldsymbol{w} \in [H_0^1(\Omega)]^2$ such that

$$\|p-p^h\|^2 = (\nabla\cdot\boldsymbol{w}, p-p^h), \quad \text{and} \quad |\boldsymbol{w}|_1 \le C\|p-p^h\|. \tag{4.14}$$

Let $\boldsymbol{e} = \boldsymbol{u}-\boldsymbol{u}^h$ and $\boldsymbol{w}^I \in \boldsymbol{V}^h$ be a piecewise polynomial interpolation of $\boldsymbol{w}$ such that

$$|\boldsymbol{w}-\boldsymbol{w}^I|_{s,K} \lesssim h_K^{1-s}|\boldsymbol{w}|_{1,K} \quad \forall K\in\mathcal{T}_h, \quad 0\le s\le 1,$$

and $\boldsymbol{w}^I = 0$ on Γ. Recalling (3.36), we have

$$\begin{aligned}
B_h(\boldsymbol{w}, p-p^h) =& B_h(\boldsymbol{w}-\boldsymbol{w}^I, p-p^h) + B_h(\boldsymbol{w}^I, p-p^h)\\
=& B_h(\boldsymbol{w}-\boldsymbol{w}^I, p-p^h) - A_h(\boldsymbol{e}, \boldsymbol{w}^I)\\
=& B_h(\boldsymbol{w}-\boldsymbol{w}^I, p-p^h) + A_h(\boldsymbol{e}, \boldsymbol{w}-\boldsymbol{w}^I) - A_h(\boldsymbol{e}, \boldsymbol{w}).
\end{aligned}$$

Based on the definitions of the bilinear forms A_h and B_h, we rewrite each term by integration by part formula and (3.1)–(3.2) as

$$\begin{aligned}
B_h(\boldsymbol{w}-\boldsymbol{w}^I, p-p^h) &= -\int_\Omega (p-p^h)\,\mathrm{div}^h(\boldsymbol{w}-\boldsymbol{w}^I)\,dx + \int_{\mathcal{E}_h^0} [\boldsymbol{w}-\boldsymbol{w}^I]\{p-p^h\}\,ds\\
&= \int_\Omega \nabla_h(p-p^h)\cdot(\boldsymbol{w}-\boldsymbol{w}^I)\,dx - \int_{\mathcal{E}_h^i} [p-p^h]\cdot\{\boldsymbol{w}-\boldsymbol{w}^I\}\,ds,
\end{aligned}$$

$$\begin{aligned}
A_h(\boldsymbol{e}, \boldsymbol{w}-\boldsymbol{w}^I) =& 2\nu\Big(\int_\Omega \boldsymbol{\varepsilon}^h(\boldsymbol{e}):\boldsymbol{\varepsilon}^h(\boldsymbol{w}-\boldsymbol{w}^I)\,dx - \int_{\mathcal{E}_h^0} [\![\boldsymbol{e}]\!]:\{\boldsymbol{\varepsilon}^h(\boldsymbol{w}-\boldsymbol{w}^I)\}\,ds\\
&- \int_{\mathcal{E}_h^0} [\![\boldsymbol{w}-\boldsymbol{w}^I]\!]:\{\boldsymbol{\varepsilon}^h(\boldsymbol{e})\}\,ds + \int_{\mathcal{E}_h^0} \eta_e h_e^{-1}[\![\boldsymbol{e}]\!]:[\![\boldsymbol{w}-\boldsymbol{w}^I]\!]\,ds\Big)\\
=& 2\nu\Big(-\int_\Omega \mathrm{div}^h(\boldsymbol{\varepsilon}^h(\boldsymbol{e}))\cdot(\boldsymbol{w}-\boldsymbol{w}^I)\,dx + \int_{\mathcal{E}_h^i} [\boldsymbol{\varepsilon}^h(\boldsymbol{e})]\cdot\{\boldsymbol{w}-\boldsymbol{w}^I\}\,ds\\
&- \int_{\mathcal{E}_h^0} [\![\boldsymbol{e}]\!]:\{\boldsymbol{\varepsilon}^h(\boldsymbol{w}-\boldsymbol{w}^I)\}\,ds + \int_{\mathcal{E}_h^0} \eta_e h_e^{-1}[\![\boldsymbol{e}]\!]:[\![\boldsymbol{w}-\boldsymbol{w}^I]\!]\,ds\Big),
\end{aligned}$$

and

$$A_h(\boldsymbol{e}, \boldsymbol{w}) = 2\nu\Big(\int_\Omega \boldsymbol{\varepsilon}^h(\boldsymbol{e}):\boldsymbol{\varepsilon}^h(\boldsymbol{w})\,dx - \int_{\mathcal{E}_h^0} [\![\boldsymbol{e}]\!]:\{\boldsymbol{\varepsilon}^h(\boldsymbol{w})\}\,ds\Big).$$

Then from the above equations and (4.14), we obtain by Cauchy–Schwarz, trace and inverse inequalities

$$\begin{aligned}
&\|p-p^h\|^2 = B_h(\boldsymbol{w}, p-p^h)\\
=& \sum_{K\in\mathcal{T}_h}\int_K \boldsymbol{f} + \mathrm{div}(2\nu\boldsymbol{\varepsilon}(\boldsymbol{u}^h) - \nabla p_h)\cdot(\boldsymbol{w}-\boldsymbol{w}^I)\,dx - \int_{\mathcal{E}_h^i} [\bar{\boldsymbol{T}}^h]\cdot\{\boldsymbol{w}-\boldsymbol{w}^I\}\,ds
\end{aligned}$$

$$
\begin{aligned}
&- 2\nu\Big(\int_\Omega \boldsymbol{\varepsilon}^h(\boldsymbol{e}) : \boldsymbol{\varepsilon}^h(\boldsymbol{w})\,dx + \int_{\mathcal{E}_h^0} [\![\boldsymbol{u}^h]\!] : \{\boldsymbol{\varepsilon}^h(\boldsymbol{w}^I)\}\,ds + \int_{\mathcal{E}_h^0} \eta_e h_e^{-1} [\![\boldsymbol{u}^h]\!] : [\![\boldsymbol{w} - \boldsymbol{w}^I]\!]\,ds\Big)\\
\lesssim &\sum_{K\in\mathcal{T}_h} \|\boldsymbol{f} + \mathrm{div}(2\nu\boldsymbol{\varepsilon}(\boldsymbol{u}^h) - \nabla p_h)\|_K \|\boldsymbol{w} - \boldsymbol{w}^I\|_K - \sum_{e\in\mathcal{E}_h^i} \|[\bar{\boldsymbol{T}}^h]\|_e \|\{\boldsymbol{w} - \boldsymbol{w}^I\}\|_e\\
&+ \|\boldsymbol{e}\|_{h,V}\|\boldsymbol{w}\|_{h,V} + \left(\sum_{e\in\mathcal{E}_h^0} h_e^{-1}\|[\![\boldsymbol{u}^h]\!]\|_e^2\right)^{1/2} \left(\sum_{e\in\mathcal{E}_h^0} h_e \|\{\boldsymbol{\varepsilon}^h(\boldsymbol{w}^I)\}\|_e^2\right)^{1/2}\\
&+ \left(\sum_{e\in\mathcal{E}_h^0} h_e^{-1}\|[\![\boldsymbol{u}^h]\!]\|_e^2\right)^{1/2} \left(\sum_{e\in\mathcal{E}_h^0} h_e^{-1}\|[\![\boldsymbol{w} - \boldsymbol{w}^I]\!]\|_e^2\right)^{1/2}\\
\lesssim &|\boldsymbol{w}|_1 \left(\Big(\sum_{K\in\mathcal{T}_h} h_K^2 \|\boldsymbol{R}_K\|_K^2\Big)^{1/2} + \Big(\sum_{e\in\mathcal{E}_h^i} h_e \|\boldsymbol{R}_e\|_e^2\Big)^{1/2} + |\boldsymbol{u}^h|_* + \|\boldsymbol{e}\|_{h,V} \right).
\end{aligned}
$$

In the last inequality, we used the fact that $\|[\![\boldsymbol{u}^h]\!]\|_e \le C\|\lfloor\boldsymbol{u}^h\rfloor\|_e$. Hence

$$
\|p - p^h\| \lesssim \eta + \|\boldsymbol{e}\|_{h,V}. \tag{4.15}
$$

For any $\boldsymbol{v} \in \boldsymbol{V}$, we have by (3.31) that

$$
\begin{aligned}
A_h(\boldsymbol{e}, \boldsymbol{v}) =& A_h(\boldsymbol{u} - \boldsymbol{z}, \boldsymbol{v}) + A_h(\boldsymbol{z} - \boldsymbol{u}^h, \boldsymbol{v})\\
=& a(\boldsymbol{u} - \boldsymbol{z}, \boldsymbol{v}) + A_h(\boldsymbol{z} - \boldsymbol{u}^h, \boldsymbol{v})\\
=& A_h(\boldsymbol{z} - \boldsymbol{u}^h, \boldsymbol{v}) - b(\boldsymbol{v}, p - y) + \int_{\Gamma_S} g\,(\boldsymbol{\lambda}_\tau^h - \boldsymbol{\lambda}_\tau) \cdot \boldsymbol{v}_\tau\, ds.
\end{aligned}
$$

By the definition of the bilinear form A_h and $[\![\boldsymbol{v}]\!] = 0$ on $\mathcal{E}_h^0$, we get

$$
\begin{aligned}
&2\nu\Big(\int_\Omega \boldsymbol{\varepsilon}^h(\boldsymbol{u} - \boldsymbol{u}^h) : \boldsymbol{\varepsilon}^h(\boldsymbol{v})\,dx - \int_{\mathcal{E}_h^0} [\![\boldsymbol{u} - \boldsymbol{u}^h]\!] : \{\boldsymbol{\varepsilon}^h(\boldsymbol{v})\}\,ds\Big)\\
=&2\nu\Big(\int_\Omega \boldsymbol{\varepsilon}^h(\boldsymbol{z} - \boldsymbol{u}^h) : \boldsymbol{\varepsilon}^h(\boldsymbol{v})\,dx - \int_{\mathcal{E}_h^0} [\![\boldsymbol{z} - \boldsymbol{u}^h]\!] : \{\boldsymbol{\varepsilon}^h(\boldsymbol{v})\}\,ds\Big)\\
&- b(\boldsymbol{v}, p - y) + \int_{\Gamma_S} g\,(\boldsymbol{\lambda}_\tau^h - \boldsymbol{\lambda}_\tau) \cdot \boldsymbol{v}_\tau\, ds.
\end{aligned}
$$

Due to the fact that $[\![\boldsymbol{u} - \boldsymbol{z}]\!] = 0$ on $\mathcal{E}_h^0$, the above equation reduces to

$$
\tilde{a}(\boldsymbol{u} - \boldsymbol{u}^h, \boldsymbol{v}) = \tilde{a}(\boldsymbol{z} - \boldsymbol{u}^h, \boldsymbol{v}) - b(\boldsymbol{v}, p - y) + \int_{\Gamma_S} g\,(\boldsymbol{\lambda}_\tau^h - \boldsymbol{\lambda}_\tau) \cdot \boldsymbol{v}_\tau\, ds, \tag{4.16}
$$

where

$$
\tilde{a}(\boldsymbol{u}, \boldsymbol{v}) = 2\nu \int_\Omega \boldsymbol{\varepsilon}^h(\boldsymbol{u}) : \boldsymbol{\varepsilon}^h(\boldsymbol{v})\,dx.
$$

As discussed in Section 4.1, let $\boldsymbol{u}^* = \mathbb{P}\boldsymbol{u}^h \in \boldsymbol{V}$ be a divergence free function constructed from $\boldsymbol{u}^h$ such that $b(\boldsymbol{u}^*, q) = 0$ for any $q \in Q$. Set $\boldsymbol{v} = \boldsymbol{u} - \boldsymbol{u}^h + \boldsymbol{u}^h - \boldsymbol{u}^*$ in (4.16); we obtain

$$
\begin{aligned}
\|\boldsymbol{e}\|_{h,V}^2 \le& \|\boldsymbol{z} - \boldsymbol{u}^h\|_{h,V}(\|\boldsymbol{e}\|_{h,V} + \|\boldsymbol{u}^h - \boldsymbol{u}^*\|_{h,V}) + \|\boldsymbol{e}\|_{h,V}\|\boldsymbol{u}^h - \boldsymbol{u}^*\|_{h,V}\\
&+ \int_{\Gamma_S} g\,(\boldsymbol{\lambda}_\tau^h - \boldsymbol{\lambda}_\tau) \cdot (\boldsymbol{u}_\tau - \boldsymbol{u}_\tau^*)\,ds\\
=& \|\boldsymbol{e}\|_{h,V}(\|\boldsymbol{z} - \boldsymbol{u}^h\|_{h,V} + \|\boldsymbol{u}^h - \boldsymbol{u}^*\|_{h,V}) + \|\boldsymbol{z} - \boldsymbol{u}^h\|_{h,V}\|\boldsymbol{u}^h - \boldsymbol{u}^*\|_{h,V}\\
&+ \int_{\Gamma_S} g\,(\boldsymbol{\lambda}_\tau^h - \boldsymbol{\lambda}_\tau) \cdot (\boldsymbol{u}_\tau - \boldsymbol{u}_\tau^*)\,ds\\
\le& \frac{1}{2}\|\boldsymbol{e}\|_{h,V}^2 + \frac{3}{2}\|\boldsymbol{z} - \boldsymbol{u}^h\|_{h,V}^2 + \frac{3}{2}\|\boldsymbol{u}^h - \boldsymbol{u}^*\|_{h,V}^2 + \int_{\Gamma_S} g\,(\boldsymbol{\lambda}_\tau^h - \boldsymbol{\lambda}_\tau) \cdot (\boldsymbol{u}_\tau - \boldsymbol{u}_\tau^*)\,ds.
\end{aligned}
$$

By the properties of $\boldsymbol{\lambda}_\tau$ (2.13) and $\boldsymbol{\lambda}_\tau^h$ (3.25),

$$\begin{aligned}\int_{\Gamma_S} g\,(\boldsymbol{\lambda}_\tau^h-\boldsymbol{\lambda}_\tau)\cdot(\boldsymbol{u}_\tau-\boldsymbol{u}_\tau^h)\,ds &= \int_{\Gamma_S} g\,(\boldsymbol{\lambda}_\tau^h\cdot\boldsymbol{u}_\tau-\boldsymbol{\lambda}_\tau^h\cdot\boldsymbol{u}_\tau^h-\boldsymbol{\lambda}_\tau\cdot\boldsymbol{u}_\tau+\boldsymbol{\lambda}_\tau\cdot\boldsymbol{u}_\tau^h)\,ds\\ &\le \int_{\Gamma_S} g\,(|\boldsymbol{u}_\tau|-|\boldsymbol{u}_\tau^h|-|\boldsymbol{u}_\tau|+|\boldsymbol{u}_\tau^h|)\,ds=0.\end{aligned}$$

In addition,

$$\begin{aligned}\int_{\Gamma_S} g\,(\boldsymbol{\lambda}_\tau^h-\boldsymbol{\lambda}_\tau)\cdot(\boldsymbol{u}_\tau^h-\boldsymbol{u}_\tau^*)\,ds &\le |\boldsymbol{\lambda}_\tau^h-\boldsymbol{\lambda}_\tau|_{*,\Gamma_S}\|\boldsymbol{u}^h-\boldsymbol{u}^*\|_{h,V}\\ &\le \epsilon|\boldsymbol{\lambda}_\tau^h-\boldsymbol{\lambda}_\tau|_{*,\Gamma_S}^2+\frac{1}{4\epsilon}\|\boldsymbol{u}^h-\boldsymbol{u}^*\|_{h,V}^2.\end{aligned}$$

Therefore, we derive

$$\|\boldsymbol{e}\|_{h,V}^2 \le 3\|\boldsymbol{z}-\boldsymbol{u}^h\|_{h,V}^2+3\|\boldsymbol{u}^h-\boldsymbol{u}^*\|_{h,V}^2+2\epsilon|\boldsymbol{\lambda}_\tau^h-\boldsymbol{\lambda}_\tau|_{*,\Gamma_S}^2+\frac{1}{2\epsilon}\|\boldsymbol{u}^h-\boldsymbol{u}^*\|_{h,V}^2. \tag{4.17}$$

By (4.15), (4.17) and recalling (3.33), we have

$$\begin{aligned}|\boldsymbol{\lambda}_\tau-\boldsymbol{\lambda}_\tau^h|_{*,\Gamma_S} &\lesssim \|\boldsymbol{u}-\boldsymbol{u}^h\|_{h,V}+\|p-p^h\|+\|\boldsymbol{u}^h-\boldsymbol{z}\|_{h,V}+\|p^h-y\|\\ &\lesssim \eta+\|\boldsymbol{u}-\boldsymbol{u}^h\|_{h,V}+\|\boldsymbol{u}^h-\boldsymbol{z}\|_{h,V}+\|p^h-y\|\\ &\lesssim \eta+\|\boldsymbol{u}^h-\boldsymbol{z}\|_{h,V}+\|p^h-y\|+\epsilon|\boldsymbol{\lambda}_\tau^h-\boldsymbol{\lambda}_\tau|_{*,\Gamma_S}.\end{aligned}$$

Hence, we obtain

$$|\boldsymbol{\lambda}_\tau-\boldsymbol{\lambda}_\tau^h|_{*,\Gamma_S} \lesssim \eta+\|\boldsymbol{z}-\boldsymbol{u}^h\|_{h,V}+\|y-p^h\|. \tag{4.18}$$

Finally, by (4.15), (4.17) and recalling (3.33), we finish the proof. ■

In the following lemma, we bound $\|\boldsymbol{z}-\boldsymbol{u}^h\|_{h,V}+\|y-p^h\|$.

Lemma 4.6.

$$\|\boldsymbol{z}-\boldsymbol{u}^h\|_{h,V}+\|y-p^h\| \lesssim \eta. \tag{4.19}$$

Proof. By an argument similar to that in proving (4.15), we can derive that

$$\|y-p^h\| \lesssim \|\boldsymbol{z}-\boldsymbol{u}^h\|_{h,V}+\eta. \tag{4.20}$$

Let $\boldsymbol{e}^* = \boldsymbol{z}-\boldsymbol{u}^* = \boldsymbol{z}-\boldsymbol{u}^h+\boldsymbol{u}^h-\boldsymbol{u}^* := \boldsymbol{\xi}+\boldsymbol{\zeta}$, and $\boldsymbol{e}^I \in \boldsymbol{V}^h$ be a piecewise polynomial interpolation of $\boldsymbol{e}^*$ such that $\boldsymbol{e}^I=0$ on Γ_D, $e_n^I=0$ on Γ_S, and

$$|\boldsymbol{e}^*-\boldsymbol{e}^I|_{s,K} \lesssim h_K^{1-s}|\boldsymbol{e}^*|_{1,K}\quad \forall K\in\mathcal{T}_h,\quad 0\le s\le 1.$$

By (3.37), we have

$$\begin{aligned}A_h(\boldsymbol{e}^*,\boldsymbol{e}^*) &= A_h(\boldsymbol{e}^*,\boldsymbol{e}^*-\boldsymbol{e}^I)+A_h(\boldsymbol{\xi},\boldsymbol{e}^I)+A_h(\boldsymbol{\zeta},\boldsymbol{e}^I)\\ &= A_h(\boldsymbol{e}^*,\boldsymbol{e}^*-\boldsymbol{e}^I)-B_h(\boldsymbol{e}^I,y-p^h)+A_h(\boldsymbol{\zeta},\boldsymbol{e}^I)\\ &= A_h(\boldsymbol{e}^*,\boldsymbol{e}^*-\boldsymbol{e}^I)+B_h(\boldsymbol{e}^*-\boldsymbol{e}^I,y-p^h)-B_h(\boldsymbol{e}^*,y-p^h)+A_h(\boldsymbol{\zeta},\boldsymbol{e}^I).\end{aligned}$$

Then let us analyze the above equality term by term. Note that $[\![\boldsymbol{e}^*]\!]=0$ on $\mathcal{E}_h^0$. By integration by part formula, we get

$$\begin{aligned}A_h(\boldsymbol{e}^*,\boldsymbol{e}^*-\boldsymbol{e}^I) &= 2\nu\int_\Omega \boldsymbol{\varepsilon}^h(\boldsymbol{\xi}):\boldsymbol{\varepsilon}^h(\boldsymbol{e}^*-\boldsymbol{e}^I)\,dx+2\nu\int_\Omega \boldsymbol{\varepsilon}^h(\boldsymbol{\zeta}):\boldsymbol{\varepsilon}^h(\boldsymbol{e}^*-\boldsymbol{e}^I)\,dx\\ &\quad -2\nu\int_{\mathcal{E}_h^0}[\![\boldsymbol{e}^*-\boldsymbol{e}^I]\!]:\{\boldsymbol{\varepsilon}^h(\boldsymbol{e}^*)\}\,ds\\ &= -\int_\Omega \mathrm{div}^h(2\nu\boldsymbol{\varepsilon}^h(\boldsymbol{\xi}))\cdot(\boldsymbol{e}^*-\boldsymbol{e}^I)\,dx+2\nu\int_{\mathcal{E}_h^i\cup\mathcal{E}_h^S}[\boldsymbol{\varepsilon}^h(\boldsymbol{\xi})]\cdot\{\boldsymbol{e}^*-\boldsymbol{e}^I\}\,ds\\ &\quad +2\nu\int_{\mathcal{E}_h^0}[\![\boldsymbol{e}^I]\!]:\{\boldsymbol{\varepsilon}^h(\boldsymbol{\zeta})\}\,ds+2\nu\int_\Omega \boldsymbol{\varepsilon}^h(\boldsymbol{\zeta}):\boldsymbol{\varepsilon}^h(\boldsymbol{e}^*-\boldsymbol{e}^I)\,dx,\end{aligned}$$

$$
\begin{aligned}
A_h(\boldsymbol{\zeta}, \boldsymbol{e}^I) :=& 2\nu\Big(\int_\Omega \boldsymbol{\varepsilon}^h(\boldsymbol{\zeta}) : \boldsymbol{\varepsilon}^h(\boldsymbol{e}^I)\,dx - \int_{\mathcal{E}_h^0} [\![\boldsymbol{\zeta}]\!] : \{\boldsymbol{\varepsilon}^h(\boldsymbol{e}^I)\}\,ds \\
&- \int_{\mathcal{E}_h^0} [\![\boldsymbol{e}^I]\!] : \{\boldsymbol{\varepsilon}^h(\boldsymbol{\zeta})\}\,ds + \int_{\mathcal{E}_h^0} \eta_e h_e^{-1} [\![\boldsymbol{\zeta}]\!] : [\![\boldsymbol{e}^* - \boldsymbol{e}^I]\!]\,ds\Big),
\end{aligned} \tag{4.21}
$$

and

$$
\begin{aligned}
B_h(\boldsymbol{e}^* - \boldsymbol{e}^I, y - p^h) &= -\int_\Omega (y - p^h)\,\mathrm{div}^h(\boldsymbol{e}^* - \boldsymbol{e}^I)\,dx + \int_{\mathcal{E}_h^0} [\boldsymbol{e}^* - \boldsymbol{e}^I]\{y - p^h\}\,ds \\
&= \int_\Omega \nabla_h(y - p^h)\cdot(\boldsymbol{e}^* - \boldsymbol{e}^I)\,dx - \int_{\mathcal{E}_h^i \cup \mathcal{E}_h^S} [y - p^h]\cdot\{\boldsymbol{e}^* - \boldsymbol{e}^I\}\,ds.
\end{aligned}
$$

Since $\boldsymbol{e}^* = \boldsymbol{z} - \boldsymbol{u}^*$ is divergence free, $B_h(\boldsymbol{e}^*, y - p^h) = 0$.

Combining the above equality together and applying the approximation property of $\boldsymbol{e}^I$, we obtain by trace and inverse inequalities

$$
\begin{aligned}
&\|\boldsymbol{e}^*\|_{h,V}^2 = A_h(\boldsymbol{e}^*, \boldsymbol{e}^*) \\
=& \sum_{K\in\mathcal{T}_h} \int_K \boldsymbol{R}_K \cdot (\boldsymbol{e}^* - \boldsymbol{e}^I)\,dx - \sum_{e\in\mathcal{E}_h^i\cup\mathcal{E}_h^S} \int_e \boldsymbol{R}_e \cdot \{\boldsymbol{w} - \boldsymbol{w}^I\}\,ds \\
&+ 2\nu\Big(\int_\Omega \boldsymbol{\varepsilon}^h(\boldsymbol{\zeta}) : \boldsymbol{\varepsilon}^h(\boldsymbol{e}^*)\,dx - 2\int_{\mathcal{E}_h^0} [\![\boldsymbol{u}^h]\!] : \{\boldsymbol{\varepsilon}^h(\boldsymbol{e}^I)\}\,ds + \int_{\mathcal{E}_h^0} \eta_e h_e^{-1} [\![\boldsymbol{u}^h]\!] : [\![\boldsymbol{e}^* - \boldsymbol{e}^I]\!]\,ds\Big) \\
\lesssim& \eta \|\boldsymbol{e}^*\|_{h,V}.
\end{aligned}
$$

So, we obtain

$$
\|\boldsymbol{e}^*\|_{h,V} \lesssim \eta.
$$

Then, by triangle inequality and (4.20), we obtain (4.19). ■

The proof of Theorem 4.4 can be completed by applying Lemmas 4.5–4.6.

4.3. Efficiency of the local error estimators

In this subsection, we consider the efficiency of the local error estimators,

$$
\eta_K = h_K \|\boldsymbol{R}_K\|_K + \Big(\sum_{e\in\mathcal{E}(K)} h_e \|\boldsymbol{R}_e\|_e^2\Big)^{1/2} + \Big(\sum_{e\in\mathcal{E}(K)} h_e^{-1} \|\lfloor \boldsymbol{u}^h \rfloor\|_e^2\Big)^{1/2}. \tag{4.22}
$$

For this purpose, following the ideas in [61,62], we make use of the bubble functions on polygonal element $K \in \mathcal{T}_h$ and edge $e \in \mathcal{E}_h$. For each polygonal element K, by assumption A3, we know that there exists a uniformly shape regular and quasi-uniform triangulation $\mathcal{T}_h^K$. Let φ_K be constructed piecewise as the sum of the classical barycentric bubble functions on $\mathcal{T}_h^K$ and τ_e be the standard edge bubble functions on $e \in \mathcal{E}_h$. Then we have the following lemma.

Lemma 4.7 ([61,62]). *For each $K \in \mathcal{T}_h$ and $e \subset \partial K$, let φ_K and τ_e be the corresponding bubble functions, respectively. Let $[P(K)]^2 \subset [H^1(K)]^2$ and $[P(e)]^2 \subset [H^1(e)]^2$ be finite-dimensional spaces of functions defined on K or e. Then*

$$
\begin{aligned}
\|\boldsymbol{v}\|_K^2 \lesssim \int_K \varphi_K \boldsymbol{v}^2\,dx \lesssim \|\boldsymbol{v}\|_K^2 \quad &\forall \boldsymbol{v} \in [P(K)]^2, \\
\|\boldsymbol{v}\|_K \lesssim \|\varphi_K \boldsymbol{v}\|_K + h_K |\varphi_K \boldsymbol{v}|_{1,K} \lesssim \|\boldsymbol{v}\|_K \quad &\forall \boldsymbol{v} \in [P(K)]^2, \\
\|\boldsymbol{v}\|_e^2 \lesssim \int_e \tau_e \boldsymbol{v}^2\,ds \lesssim \|\boldsymbol{v}\|_e^2 \quad &\forall \boldsymbol{v} \in [P(e)]^2, \\
h_K^{-1/2} \|\tau_e \boldsymbol{v}\|_K + h_K^{1/2} |\tau_e \boldsymbol{v}|_{1,K} \lesssim \|\boldsymbol{v}\|_e \quad &\forall \boldsymbol{v} \in [P(e)]^2.
\end{aligned}
$$

Following the ideas in [51,63], we first give the residual equation. Recall (4.16) and (3.29), for any $\boldsymbol{v} \in \boldsymbol{V}$, we have

$$
\begin{aligned}
&\tilde{a}(\boldsymbol{u} - \boldsymbol{u}^h, \boldsymbol{v}) + b(\boldsymbol{v}, p - p^h) \\
=& a(\boldsymbol{z}, \boldsymbol{v}) + b(\boldsymbol{v}, y) - \tilde{a}(\boldsymbol{u}^h, \boldsymbol{v}) - b(\boldsymbol{v}, p^h) + \int_{\Gamma_S} g\,(\boldsymbol{\lambda}_\tau^h - \boldsymbol{\lambda}_\tau)\cdot \boldsymbol{v}_\tau\,ds \\
=& \ell^h(\boldsymbol{v}) + \sum_{K\in\mathcal{T}_h} \int_K (\mathrm{div}(2\nu\boldsymbol{\varepsilon}^h(\boldsymbol{u}^h)) - \nabla p^h)\cdot \boldsymbol{v}\,dx
\end{aligned}
$$

$$
\begin{aligned}
& - \int_{\mathcal{E}_h^i \cup \mathcal{E}_h^S} [2\nu \boldsymbol{\varepsilon}^h(\boldsymbol{u}^h) - p^h \mathbf{I}] \cdot \{\boldsymbol{v}\}\, ds + \int_{\Gamma_S} g\,(\boldsymbol{\lambda}_\tau^h - \boldsymbol{\lambda}_\tau) \cdot \boldsymbol{v}_\tau\, ds \\
&= \sum_{K \in \mathcal{T}_h} \int_K \boldsymbol{R}_K \cdot \boldsymbol{v}\, dx - \int_{\mathcal{E}_h^i \cup \mathcal{E}_h^S} \boldsymbol{R}_e \cdot \boldsymbol{v}\, ds + \int_{\Gamma_S} g\,(\boldsymbol{\lambda}_\tau^h - \boldsymbol{\lambda}_\tau) \cdot \boldsymbol{v}_\tau\, ds. \qquad (4.23)
\end{aligned}
$$

Let $\bar{\boldsymbol{R}}_K$ be an approximation to the residual $\boldsymbol{R}_K$ from a suitable finite-dimensional subspace $[P(K)]^2$. Note that φ_K vanishes on the boundary of K, so it can be extended to be zero on the rest of domain as a continuous function. Let $\boldsymbol{v} = \bar{\boldsymbol{R}}_K \varphi_K$ in (4.23). By a standard argument, we have

$$
\|\boldsymbol{R}_K\|_K \lesssim h_K^{-1} \|\boldsymbol{u} - \boldsymbol{u}^h\|_{K,V} + h_K^{-1} \|p - p^h\|_K + \|\boldsymbol{R}_K - \bar{\boldsymbol{R}}_K\|_K. \qquad (4.24)
$$

For the residual $\boldsymbol{R}_e$, set $\bar{\boldsymbol{R}}_e$ be its approximation from $[P(e)]^2$. Because τ_e vanishes on the boundary of ω_e, similarly, we can extend it to be zero on the rest of domain as a continuous function. For $e \in \mathcal{E}_h^S$, choose $\boldsymbol{v} = \bar{\boldsymbol{R}}_e \tau_e$ in (4.23), we have

$$
\begin{aligned}
& \int_{\omega_e} \boldsymbol{\varepsilon}^h(\boldsymbol{u} - \boldsymbol{u}^h) : \boldsymbol{\varepsilon}^h(\bar{\boldsymbol{R}}_e \tau_e)\, dx - \int_{\omega_e} (p - p^h)\, \mathrm{div}(\bar{\boldsymbol{R}}_e \tau_e)\, dx \\
&= \int_{\omega_e} \boldsymbol{R}_K \cdot \bar{\boldsymbol{R}}_e \tau_e\, dx - \int_e \boldsymbol{R}_e \cdot \bar{\boldsymbol{R}}_e \tau_e\, ds + \int_e g\,(\boldsymbol{\lambda}_\tau^h - \boldsymbol{\lambda}_\tau) \cdot (\bar{\boldsymbol{R}}_e \tau_e)_\tau\, ds \\
&= \int_{\omega_e} \boldsymbol{R}_K \cdot \bar{\boldsymbol{R}}_e \tau_e\, dx - \int_e (\boldsymbol{R}_e - \bar{\boldsymbol{R}}_e) \cdot \bar{\boldsymbol{R}}_e \tau_e\, ds - \int_e \bar{\boldsymbol{R}}_e \cdot \bar{\boldsymbol{R}}_e \tau_e\, ds + \int_e g\,(\boldsymbol{\lambda}_\tau^h - \boldsymbol{\lambda}_\tau) \cdot (\bar{\boldsymbol{R}}_e \tau_e)_\tau\, ds.
\end{aligned}
$$

Then by Lemma 4.7, we get

$$
\begin{aligned}
& \|\bar{\boldsymbol{R}}_e\|_e^2 \lesssim \int_e \bar{\boldsymbol{R}}_e \cdot \bar{\boldsymbol{R}}_e \tau_e\, ds \\
\le & (\|\boldsymbol{u} - \boldsymbol{u}^h\|_{\omega_e,V} + \|p - p^h\|_{\omega_e}) |\bar{\boldsymbol{R}}_e \tau_e|_{1,\omega_e} + \|\boldsymbol{R}_K\|_{0,\omega_e} \|\bar{\boldsymbol{R}}_e \tau_e\|_{0,\omega_e} \\
& + \|\boldsymbol{R}_e - \bar{\boldsymbol{R}}_e\|_e \|\bar{\boldsymbol{R}}_e \tau_e\|_e + |\boldsymbol{\lambda}_\tau^h - \boldsymbol{\lambda}_\tau|_{*,e} |\bar{\boldsymbol{R}}_e \tau_e|_{1,\omega_e} \\
\lesssim & h_K^{-1/2} (\|\boldsymbol{u} - \boldsymbol{u}^h\|_{\omega_e,V} + \|p - p^h\|_{\omega_e} + |\boldsymbol{\lambda}_\tau - \boldsymbol{\lambda}_\tau^h|_{*,e}) \|\bar{\boldsymbol{R}}_e\|_e + h_K^{1/2} \|\boldsymbol{R}_K\|_{0,\omega_e} \|\bar{\boldsymbol{R}}_e\|_e \\
& + \|\boldsymbol{R}_e - \bar{\boldsymbol{R}}_e\|_e \|\bar{\boldsymbol{R}}_e\|_e.
\end{aligned}
$$

Hence, by the triangle inequality and (4.24), we obtain

$$
\begin{aligned}
\|\boldsymbol{R}_e\|_e \lesssim & h_K^{-1/2} \left(\|\boldsymbol{u} - \boldsymbol{u}^h\|_{\omega_e,V} + \|p - p^h\|_{\omega_e} + |\boldsymbol{\lambda}_\tau - \boldsymbol{\lambda}_\tau^h|_{*,e} \right) \\
& + h_K^{1/2} \|\boldsymbol{R}_K - \bar{\boldsymbol{R}}_K\|_{\omega_e} + \|\boldsymbol{R}_e - \bar{\boldsymbol{R}}_e\|_e. \qquad (4.25)
\end{aligned}
$$

In addition, for $e \in \mathcal{E}_h^i$, choose $\boldsymbol{v} = \bar{\boldsymbol{R}}_e \tau_e$ in (4.23) and by similar argument, we can derive

$$
\|\boldsymbol{R}_e\|_e \lesssim h_K^{-1/2} \left(\|\boldsymbol{u} - \boldsymbol{u}^h\|_{\omega_e,V} + \|p - p^h\|_{\omega_e} \right) + h_K^{1/2} \|\boldsymbol{R}_K - \bar{\boldsymbol{R}}_K\|_{\omega_e} + \|\boldsymbol{R}_e - \bar{\boldsymbol{R}}_e\|_e. \qquad (4.26)
$$

Note that $\mathrm{div}(2\nu \boldsymbol{\varepsilon}(\boldsymbol{u}^h)) - \nabla p_h$ is a polynomial in K and so is $[2\nu \boldsymbol{\varepsilon}(\boldsymbol{u}^h) - p^h \boldsymbol{I}]$ on e. Hence, the terms $\|\boldsymbol{R}_K - \overline{\boldsymbol{R}}_K\|_K$ and $\|\boldsymbol{R}_e - \overline{\boldsymbol{R}}_e\|_e$ can be replaced by $\|\boldsymbol{f} - \bar{\boldsymbol{f}}\|_K$ and $\|\boldsymbol{\lambda}_\tau^h - \overline{\boldsymbol{\lambda}}_\tau^h\|_e$, with discontinuous piecewise polynomial approximations $\overline{\boldsymbol{\lambda}}_\tau^h$.

By trace inequality, we have

$$
h_e^{-1/2} \|\lfloor \boldsymbol{u}^h \rfloor\|_e \lesssim h_e^{-1} \|\boldsymbol{u} - \boldsymbol{u}^h\|_{\omega_e} + \|\nabla(\boldsymbol{u} - \boldsymbol{u}^h)\|_{\omega_e}. \qquad (4.27)
$$

Note that the extra term $h_e^{-1} \|\boldsymbol{u} - \boldsymbol{u}^h\|_{\omega_e}$ is not desirable, however, this term is expected to be of the same order as $\|\nabla(\boldsymbol{u} - \boldsymbol{u}^h)\|_{\omega_e}$.

Combining (4.24), (4.25), (4.26) and (4.27), we obtain a lower bound of the local error indicator defined in (4.22).

Theorem 4.8. *Let $(\boldsymbol{u}, p, \boldsymbol{\lambda}_\tau)$ be the solution of (2.13), and let $(\boldsymbol{u}^h, p^h, \boldsymbol{\lambda}_\tau^h)$ be the solution of (3.23)–(3.25). Then the local estimator (4.22) satisfies*

$$
\begin{aligned}
\eta_K \lesssim & \|\boldsymbol{u} - \boldsymbol{u}^h\|_{\omega_K,V} + \|p - p^h\|_{\omega_K} + \sum_{e \in \mathcal{E}(K) \cap \mathcal{E}_h^S} |\boldsymbol{\lambda}_\tau - \boldsymbol{\lambda}_\tau^h|_{*,e} \\
& + h_K \|\boldsymbol{f} - \bar{\boldsymbol{f}}\|_{\omega_K} + \sum_{e \in \mathcal{E}(K) \cap \mathcal{E}_h^S} h_e \|\boldsymbol{\lambda}_\tau^h - \overline{\boldsymbol{\lambda}}_\tau^h\|_e^2 + h_K^{-1} \|\boldsymbol{u} - \boldsymbol{u}^h\|_{\omega_K}. \qquad (4.28)
\end{aligned}
$$

5. Numerical examples

Given an initial mesh $\mathcal{T}_0$, each loop of the h-adaptive algorithm consists of four steps as shown in Fig. 1.

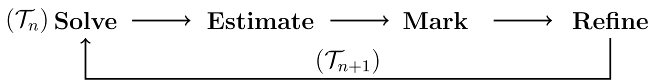

Fig. 1. Loop of h-adaptive algorithm.

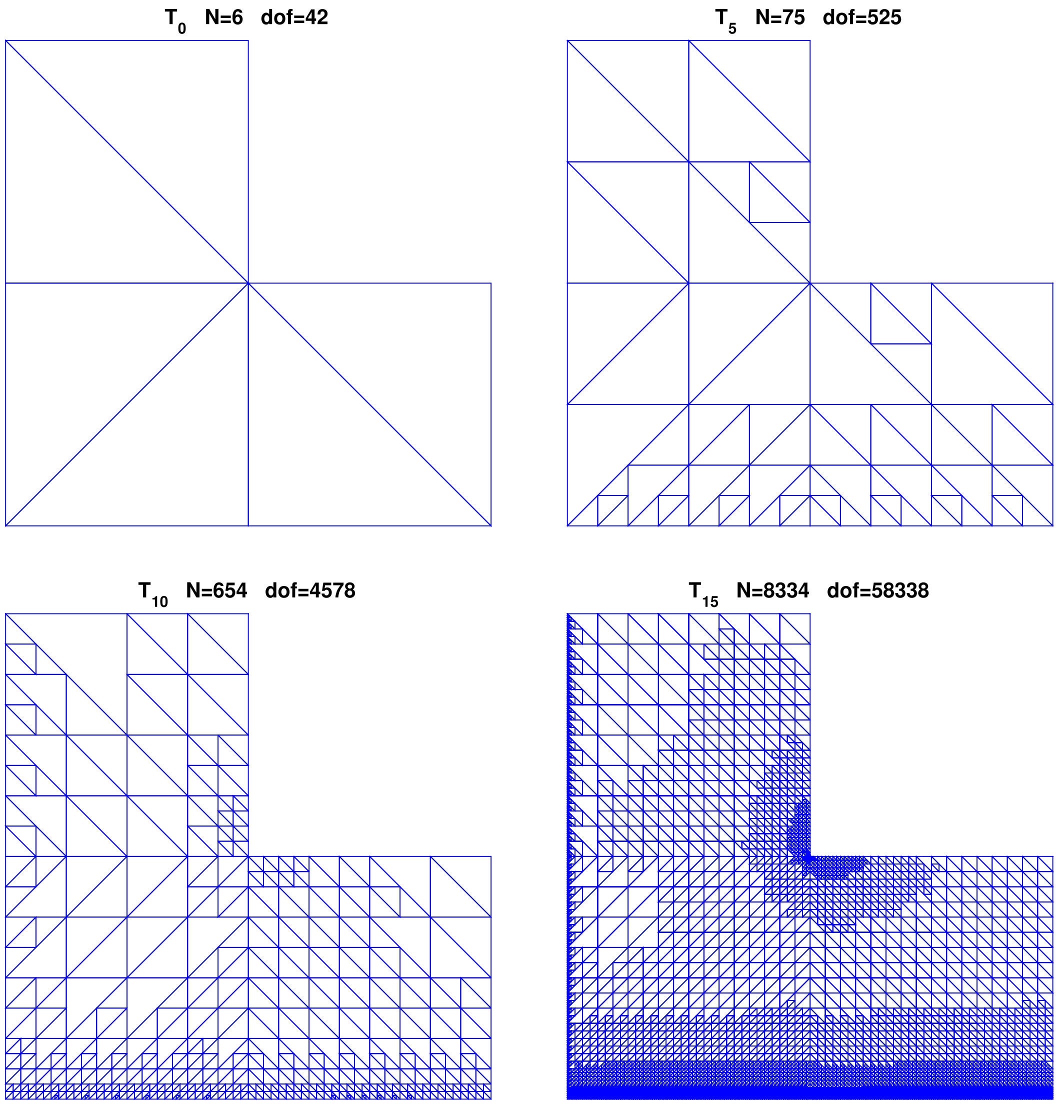

Fig. 2. Adaptively refined meshes in Example 1.

In each loop, solve the problem by the DG method on the mesh $\mathcal{T}_n$ first. Next, based on the a posteriori error analysis, we choose the error indicator as the local error estimator (4.22). Then we mark the elements to be refined by the bulk criterion strategy

$$\sum_{K\in\mathcal{M}_h} \eta_K \geq \theta \sum_{K\in\mathcal{T}_h} \eta_K, \qquad 0<\theta<1. \tag{5.1}$$

The elements are sorted according to the values of the local error indicators, i.e., elements with larger errors are placed into the marked set $\mathcal{M}_h$ until the inequality (5.1) is satisfied. Finally, the marked elements are refined to obtain a new mesh $\mathcal{T}_{n+1}$. To refine the elements in $\mathcal{M}_h$, midpoints on the three edges are connected to divide the element into four new elements. Note that hanging nodes are allowed for DG methods, so additional subdivisions to eliminate the hanging nodes are not needed.

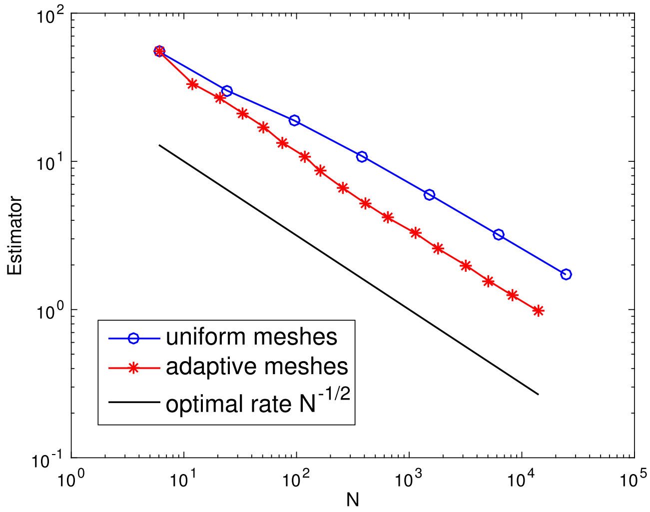

Fig. 3. Convergence rate in Example 1.

Table 3
Order of convergence for adaptively refined meshes in Example 1.

N	dof	Estimator	Order
1131	7917	3.2819	–
1797	12 579	2.5784	0.5210
3153	22 071	1.9973	0.4542
5049	35 343	1.5673	0.5149
8334	58 338	1.2393	0.4685
14 097	98 679	0.9736	0.4591

In the following examples, we use the IP DG scheme with penalty parameter $\eta = 10$, and set the parameter $\theta = 0.5$ for the bulk criterion strategy. To solve the discretized problem, we adopt the Uzawa algorithm in [25].

Example 5.1. The first example is considered in an L-shape domain $\Omega = (-1, 1)^2 \setminus [0, 1]^2$ with slip boundary $\Gamma_S = \{-1\} \times (-1, 1)$ and the Dirichlet boundary $\Gamma_D = \partial\Omega \setminus \Gamma_S$, see Fig. 2. Boundary conditions are set as $\boldsymbol{u}|_{\Gamma_D} = \boldsymbol{0}$ and $u_n|_{\Gamma_S} = 0$. Let $\nu = 1$ and $g = 0.2$. The external force $\boldsymbol{f}$ is defined by

$$
\begin{aligned}
f_1(x, y) = &- \frac{3(x-0.1)^2(y-0.1)}{((x-0.1)^2+(y-0.1)^2)^{\frac{5}{2}}} - \frac{y-0.1}{((x-0.1)^2+(y-0.1)^2)^{\frac{3}{2}}} \\
&- \frac{3(y-0.1)^3}{((x-0.1)^2+(y-0.1)^2)^{\frac{5}{2}}} - \frac{3(y-0.1)}{((x-0.1)^2+(y-0.1)^2)^{\frac{3}{2}}},
\end{aligned}
$$

$$
\begin{aligned}
f_2(x, y) = &- \frac{x-0.1}{((x-0.1)^2+(y-0.1)^2)^{\frac{3}{2}}} - \frac{3(x-0.1)(y-0.1)^2}{((x-0.1)^2+(y-0.1)^2)^{\frac{5}{2}}} \\
&- \frac{3(x-0.1)}{((x-0.1)^2+(y-0.1)^2)^{\frac{3}{2}}} - \frac{3(x-0.1)^3}{((x-0.1)^2+(y-0.1)^2)^{\frac{5}{2}}} \\
&- \frac{1}{(y+1.05)^2}.
\end{aligned}
$$

Because the exact analytic solution is not available, we summarize the numerical results of the total error estimator η with respected to number of elements N and degrees of freedom (dof) for adaptively refined and uniformly refined meshes in Tables 3–4, respectively. Adaptively refined meshes are shown in Fig. 2, and error estimator is plotted with respected to number of the elements N on uniformly refined meshes and adaptively refined meshes respectively in Fig. 3. Note that the expected optimal convergence rate is $O(N^{-1/2})$.

Example 5.2. We consider a Stokes flow in a channel. The computational domain is given by $\Omega = [0, 10] \times [0, 1] \setminus [2, 2.5] \times [0, 0.5]$. We choose $\nu = 1$, $g = 0.2$ and $\boldsymbol{f} = \boldsymbol{0}$. The slip boundary Γ_S is selected as the boundary

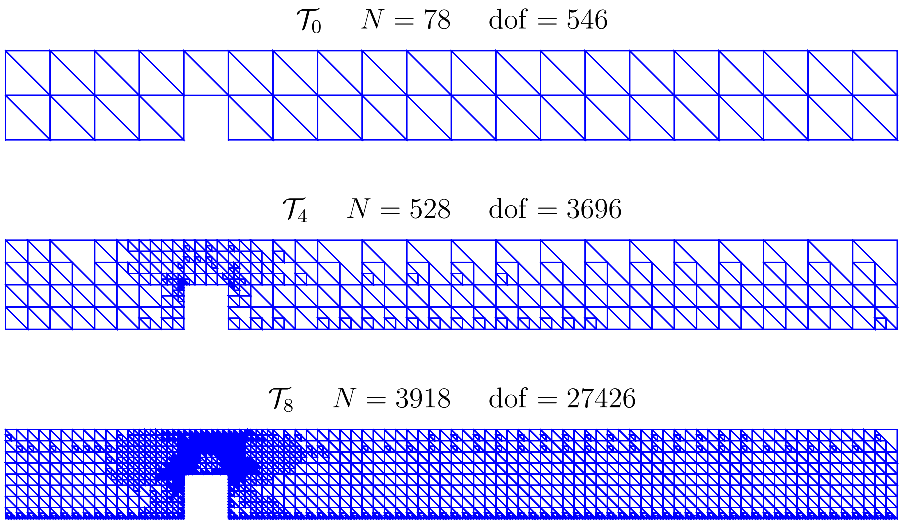

Fig. 4. Refined meshes in Example 2.

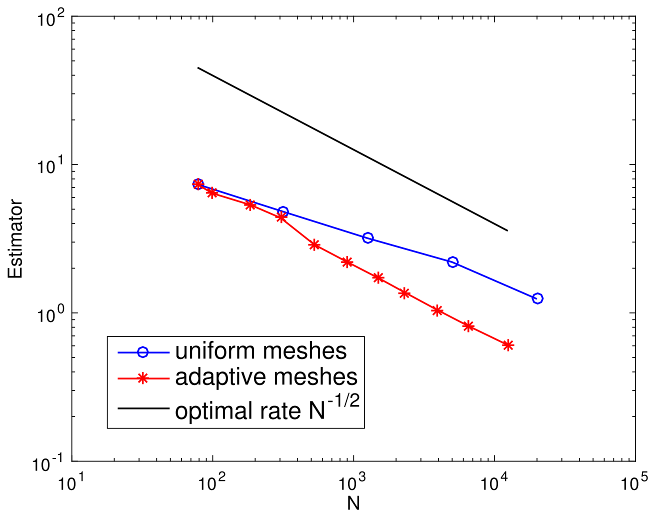

Fig. 5. Convergence rate in Example 2.

Table 4
Order of convergence for uniformly refined meshes in Example 1.

N	dof	Estimator	Order
384	2688	10.8207	–
1536	10 752	5.9337	0.4334
6144	43 008	3.2035	0.4446
24 576	172 032	1.7214	0.4480

on the bottom, the Dirichlet boundary Γ_D is the side on the top, and furthermore, set

$$\boldsymbol{u}|_{x=0} = (y(1-y), 0), \quad \boldsymbol{u}|_{y=1} = \boldsymbol{0},$$

$$\boldsymbol{u}|_{x=10} = (y(1-y), 0), \quad u_n|_{\Gamma_S} = 0.$$

In this example, we simulate the case where there is an obstacle in the channel, so the block $[2, 2.5] \times [0, 0.5]$ is cut out from the computational domain. There is no solution formula, so the numerical results of the total error estimator η are listed with respected to number of elements and degrees of freedom for adaptively refined and uniformly refined meshes in Tables 5–6, respectively. Adaptively refined meshes are shown in Fig. 4, and error estimators on uniformly refined meshes and adaptively refined meshes are plotted with respected to N in Fig. 5.

Table 5
Order of convergence for adaptively refined meshes in Example 2.

N	dof	Estimator	Order
900	6300	2.2044	–
1497	10 479	1.7185	0.4894
2313	16 191	1.3717	0.5181
3918	27 426	1.0474	0.5118
6456	45 192	0.8196	0.4911
12 413	86 891	0.6073	0.4586

Table 6
Order of convergence for uniformly refined meshes in Example 2.

N	dof	estimator	order
312	2184	4.8320	–
1248	8736	3.1918	0.2991
4992	34 944	2.2006	0.2682
19 968	139 776	1.2417	0.4128

References

[1] C. Neto, D.R. Evans, E. Bonaccurso, H.-J. Butt, V.S.J. Craig, Boundary slip in Newtonian liquids: a review of experimental studies, Rep. Progr. Phys. 68 (2005) 2859–2897.
[2] E. Lauga, M. Brenner, H. Stone, Microfluidics: the no-slip boundary condition, in: Springer Handbook of Experimental Fluid Mechanics, Springer, Berlin, Heidelberg, 2007, pp. 1219–1240.
[3] Y. Nubar, Blood flow: slip and viscometry, Biophys. J. 11 (1971) 252–264.
[4] M. Denn, Extrusion instabilities and wall slip, Annu. Rev. Fluid Mech. 33 (2001) 265–287.
[5] E.B. Arkilic, M.A. Schmidt, K. Breuer, Gaseous slip flow in long microchannels, J. Microelectromech. Syst. 6 (1997) 167–178.
[6] C. Navier, Mémoire sur les lois du mouvement des fluides, Mém. Acad. Roy. Sci. Inst. Fr. 6 (1823) 389–416.
[7] P.S. Girard, Mém. Classe Sci. Math. Phys. Inst. Fr. 14 (1815) 329.
[8] P.A. Thompson, O.R. Mark, Simulations of contact-line motion: slip and the dynamic contact angle, Phys. Rev. Lett. 63 (1989) 766.
[9] R. Pit, H. Hervet, L. Leger, Direct experimental evidence of slip in hexadecane: solid interfaces, Phys. Rev. Lett. 85 (2000) 980–983.
[10] J. Baudry, E. Charlaix, A. Tonck, D. Mazuyer, Experimental evidence for a large slip effect at a nonwetting fluid-solid interface, Langmuir 17 (2001) 5232–5236.
[11] V.S.J. Craig, C. Neto, D.R.M. Williams, Shear dependent boundary slip in an aqueous Newtonian liquid, Phys. Rev. Lett. 87 (2001) 054504.
[12] Y. Zhu, S. Granick, Rate-dependent slip of Newtonian liquids at smooth surfaces, Phys. Rev. Lett. 87 (2001) (2001) 96105.
[13] C. Wu, G. Ma, On the boundary slip of fluid flow, Sci. China Ser. G 48 (2005) 178–187.
[14] H. Fujita, Flow Problems with Unilateral Boundary Conditions, Leçons, Collège de France, 1993.
[15] H. Fujita, A mathematical analysis of motions of viscous incompressible fluid under leak or slip boundary conditions, RIMS Kokyuroku 88 (1994) 199–216.
[16] H. Fujita, Non-stationary Stokes flows under leak boundary conditions of friction type, J. Comput. Math. 19 (2001) 1–8.
[17] H. Fujita, A coherent analysis of Stokes flows under boundary conditions of friction type, J. Comput. Appl. Math. 149 (2002) 57–69.
[18] N. Saito, H. Fujita, Regularity of solutions to the Stokes equation under a certain nonlinear boundary condition, Lect. Notes Pure Appl. Math. 223 (2002) 73–86.
[19] N. Saito, On the Stokes equations with the leak and slip boundary conditions of friction type: regularity of solutions, Publ. Res. Inst. Math. Sci. 40 (2004) 345–383.
[20] R. An, K. Li, Variational inequality for the rotating Navier–Stokes equations with subdifferential boundary conditions, Comput. Math. Appl. 55 (2008) 581–587.
[21] Y. Li, K. Li, Existence of the solution to stationary Navier–Stokes equations with nonlinear slip boundary conditions, J. Math. Anal. Appl. 381 (2011) 1–9.
[22] T. Kashiwabara, On a strong solution of the non-stationary Navier–Stokes equations under slip or leak boundary conditions of friction type, J. Differential Equations 254 (2013) 756–778.
[23] Y. Li, K. Li, Pressure projection stabilized finite element method for Navier–Stokes equations with nonlinear slip boundary conditions, Computing 87 (2010) 113–133.
[24] Y. Li, R. An, Two-level pressure projection finite element methods for Navier–Stokes equations with nonlinear slip boundary conditions, Appl. Numer. Math. 61 (2011) 285–297.
[25] Y. Li, K. Li, Uzawa iteration method for Stokes type variational inequality of the second kind, Acta Math. Appl. Sin. 17 (2011) 303–316.
[26] T. Kashiwabara, On a finite element approximation of the Stokes equations under a slip boundary condition of the friction type, Japan J. of Ind. Appl. Math. 30 (2013) 227–261.
[27] R. An, Y. Li, Two-level penalty finite element methods for Navier–Stokes equations with nonlinear slip boundary conditions, Int. J. Numer. Anal. Model. 11 (2014) 608–623.
[28] F. Jing, J. Li, Z. Chen, Stabilized finite element methods for a blood flow model of arterosclerosis, Numer. Methods Partial Differential Equations 31 (2015) 2063–2079.
[29] J.K. Djoko, J. Koko, Numerical methods for the Stokes and Navier–Stokes equations driven by threhold slip boundary conditions, Comput. Methods Appl. Mech. Engrg. 305 (2016) 936–958.
[30] D.N. Arnold, F. Brezzi, B. Cockburn, L.D. Marini, Unified analysis of discontinuous Galerkin methods for elliptic problems, SIAM J. Numer. Anal. 39 (2002) 1749–1779.
[31] B. Cockburn, G.E. Karniadakis, C.-W. Shu (Eds.), Discontinuous Galerkin methods, in: Theory, Computation and Applications, in: Lecture Notes in Computational Science and Engineering, vol. 11, Springer-Verlag, New York, 2000.

[32] Q. Hong, F. Wang, S. Wu, J. Xu, A unified study of continuous and discontinuous Galerkin methods, Sci. China Math. 62 (2019) 1–32.
[33] F. Bassi, S. Rebay, A high-order accurate discontinuous finite element method for the numerical solution of the compressible Navier–Stokes equations, J. Comput. Phys. 131 (1997) 267–279.
[34] X. Ye, Discontinuous stable elements for the incompressible flow, Adv. Comput. Math. 20 (2004) 333–345.
[35] V. Girault, B. Riviere, M.F. Wheeler, A discontinuous Galerkin method with non-overlapping domain decomposition for the Stokes and Navier–Stokes problems, Math. Comp. 74 (2005) 53–84.
[36] B. Cockburn, G. Kanschat, D. Schotzau, A locally conservative LDG method for the incompressible Navier–Stokes equations, Math. Comp. 74 (2005) 1067–1095.
[37] B. Cockburn, G. Kanschat, D. Schotzau, A note on discontinuous Galerkin divergence-free solutions of the Navier–Stokes equations, J. Sci. Comput. 31 (2007) 61–73.
[38] J.K. Djoko, F. Ebobisse, A.T. McBride, B.D. Reddy, A discontinuous Galerkin formulation for classical and gradient plasticity - part 1: Formulation and analysis, Comput. Methods Appl. Mech. Engrg. 196 (2007) 3881–3897.
[39] J.K. Djoko, F. Ebobisse, A.T. McBride, B.D. Reddy, A discontinuous Galerkin formulation for classical and gradient plasticity - part 2: Algorithms and numerical analysis, Comput. Methods Appl. Mech. Engrg. 197 (2007) 1–21.
[40] F. Wang, W. Han, X. Cheng, Discontinuous Galerkin methods for solving elliptic variational inequalities, SIAM J. Numer. Anal. 48 (2010) 708–733.
[41] F. Wang, W. Han, X. Cheng, Discontinuous Galerkin methods for solving signorini problem, IMA J. Numer. Anal. 31 (2011) 1754–1772.
[42] S.C. Brenner, L. Sung, H. Zhang, Y. Zhang, A quadratic C^0 interior penalty method for the displacement obstacle problem of clamped kirchhoff plates, SIAM J. Numer. Anal. 50 (2012) 3329–3350.
[43] J.K. Djoko, Discontinuous Galerkin finite element discretization for steady Stokes flows with threshold slip boundary condition, Quaest. Math. 36 (2013) 501–516.
[44] F. Wang, W. Han, X. Cheng, Discontinuous Galerkin methods for solving a quasistatic contact problem, Numer. Math. 126 (2014) 771–800.
[45] F. Jing, W. Han, W. Yan, F. Wang, Discontinuous Galerkin finite element methods for stationary Navier–Stokes problem with a nonlinear slip boundary condition of friction type, J. Sci. Comput. 76 (2018) 888–912.
[46] F. Wang, T. Zhang, W. Han, C^0 Discontinuous Galerkin methods for a kirchhoff plate contact problem, J. Comput. Math. 37 (2019) 184–200.
[47] T. Gudi, K. Porwal, A posteriori error control of discontinuous Galerkin methods for elliptic obstacle problems, Math. Comp. 83 (2014) 579–602.
[48] T. Gudi, K. Porwal, A reliable residual based a posteriori error estimator for a quadratic finite element method for the elliptic obstacle problem, Comput. Methods Appl. Math. 15 (2015) 145–160.
[49] T. Gudi, K. Porwal, A posteriori error estimates of discontinuous Galerkin methods for the signorini problem, J. Comput. Appl. Math. 292 (2016) 257–278.
[50] F. Wang, W. Han, J. Eichholz, X. Cheng, A posteriori error estimates of discontinuous Galerkin methods for obstacle problems, Nonlinear Anal. RWA 22 (2015) 664–679.
[51] F. Wang, W. Han, Reliable and efficient a posteriori error estimates of DG methods for a frictional contact problem, Int. J. Numer. Anal. Model. 16 (2019) 49–62.
[52] J. Nečas, I. Hlavaček, Mathematical Theory of Elastic and Elastoplastic Bodies: An Introduction, Elsevier, Amsterdam, 1981.
[53] R. Glowinski, Numerical Methods for Nonlinear Variational Problems, Springer-Verlag, New York, 1984.
[54] L. Beirão da Veiga, F. Brezzi, A. Cangiani, G. Manzini, L.D. Marini, A. Russo, Basic principles of virtual element methods, Math. Models Methods Appl. Sci. 23 (2013) 119–214.
[55] L. Beirão da Veiga, C. Lovadina, A. Russo, Stability analysis for the virtual element method, Math. Models Methods Appl. Sci. 27 (2017) 2557–2594.
[56] S.C. Brenner, R.L. Scott, The Mathematical Theory of Finite Element Methods, in: Texts in Applied Mathematics, vol. 15, Springer-Verlag, 2008.
[57] L. Chen, J. Huang, Some error analysis on virtual element methods, Calcolo 55 (2018) http://dx.doi.org/10.1007/s10092-018-0249-4.
[58] M.F. Wheeler, An elliptic collocation finite element method with interior penalties, SIAM J. Numer. Anal. 15 (1978) 152–161.
[59] F. Brezzi, G. Manzini, D. Marini, P. Pietra, A. Russo, Discontinuous finite elements for diffusion problems, in: Atti Convegno in Onore Di F. Brioschi (Milan, 1997), Istituto Lombardo, Accademia di Scienze e Lettere, Milan, Italy, 1999, pp. 197–217.
[60] B. Cockburn, C.-W. Shu, The local discontinuous Galerkin method for time-dependent convection–diffusion systems, SIAM J. Numer. Anal. 35 (1998) 2440–2463.
[61] M. Ainsworth, T.J. Oden, A Posteriori Error Estimation in Finite Element Analysis, Wiley, Chichester, 2000.
[62] A. Cangiani, E.H. Georgoulis, T. Pryer, O.J. Sutton, A posteriori error estimates for the virtual element method, Numer. Math. (2017) http://dx.doi.org/10.1007/s00211-017-0891-9.
[63] F. Wang, W. Han, Another view for a posteriori error estimates for variational inequalities of the second kind, Appl. Numer. Math. 72 (2013) 225–233.